論 說 報 告

第十九卷 第一號 昭和八年一月

# STUDIES ON PHOTO-ELASTICITY

By Juichiro Kuno, Dr. Eng., Member.

## Synopsis.

1. The law of photo-elastic extinction $Sd=Kn$ is established, the constant $K$ being referred to as *the coefficient of photo-elastic extinction* (光彈性消光係數).

2. The photo-elastic phenomenon in phenolite may be interpreted as a result *caused by strain* and *not* by stress.

3. Stress *in a roller diametrically compressed* is mathematically determined by applying the theory of complex functions.

4. *A rectangular plate compressed on two sides* is considered by means of Airy's stress-function.

5. In each of these two problems, a specimen of phenolite is tested by the photo-elastic apparatus to compare the calculation with the experiment with attention to *the time effect*.

## Contents.



## INTRODUCTION.

In problems of elasticity there are many cases, in which stress distribution can be hardly found by mathematical analysis. As a useful weapon to attack such a difficult problem, chiefly of two-dimension, the photo-elastic method has been studied and applied since the beginning of this century by E. G. Coker[1], L. N. G. Filon, A. Mesnager, W. Birnbaum, Z. Tuzi, I. Arakawa, T. Fukuhara[2], K. Okuda[3] and others.

As for the fundamental nature of photo-elastic phenomenon, there has been still a question whether stress or strain is the immediate cause of the temporary double refraction. This subject was first investigated by Filon and Jessop[4] with specimens of glass and celluloid. One of the facts they found in celluloid is that the optical phenomenon due to stress undergoes considerable time effect. This result

(1) Coker and Filon's "*A Treatise on Photo-elasticity*" gives a list of papers writen in European languages dated up to 1931.

(2) *Jour. Soc. Mech. Eng.* (in Japanese), xxx, p. 336 (1927) and xxxi. p. 169 (1928).

(3) *Ditto*, xxxi, p. 350 (1928) and xxxii, p. 271 (1929).

(4) *Phil. Trans. A*, ccxxiii, p. 89 (1923).

leads to another question how the elimination of the time effect can be done in practical observation. To photograph isochromatic lines with monochromatic light may appear to answer the question, still this is insufficient if we do not care about the fact that the dark band photographed at the instant of loading differs remarkably in position from the same band taken at another instant, even though the load remains constant. Phenolite is now extensively used in this country as a new material for photo-elastic experiments, while the quantitative measurement of the time effect in this material seems to have remained untouched.

In Chapter 1 the optical effect due to the simple stress is measured by means of the BABINET'S compensator with specimens of phenolite supplied by *the Institute of Physical and Chemical Research*, Tokyo. The main object is to consider further the known relation between stress and optical effect and then to investigate the variation of the optical effect with time. Experiments described in Chapter 2 are made also with phenolite to measure the effect of time upon strain. The relation between strain and optical effect is examined in order to settle the question whether the optical effect is caused by the strain. These two chapters constitute Part I, viz., the photo-elastic behaviour of phenolite.

The two subsequent chapters in Part II are devoted to the theoretical investigation of the stress distribution in some two-dimensional problems to construct isochromatic lines, which are to be compared with experiments. In Chapter 3 stress in a roller diametrically compressed is mathematically determined by applying a method of calculation proposed by Prof. S. YOKOTA. In Chapter 4 a rectangular plate compressed on two opposite sides is considered by means of AIRY'S stress-function. In each of these problems, a specimen of phenolite is tested under polarized light to compare the calculation with the experiment with attention to the time effect.

# PART I.

# PHOTO-ELASTIC BEHAVIOUR OF PHENOLITE.

## Chapter 1. Extinction of Light in Phenolite under Stress.

### 1. Optical effect due to stress.

Since the time of Sir DAVID BREWSTER, experiments have been made that show, if an incident ray falls perpendicularly upon the plane of a transparent elastic plate strained two-dimensionally by a system of loads, the light is broken up into two components polarized in the directions of principal stresses. If the plate is placed

between crossed nicols, it is found that the light passing through a point, at which the directions of principal stresses are in the directions of principal planes of the nicols, is extinguished. This darkness depending on the directions of principal stresses we shall speak of as *the photo-elastic extinction of the first kind*. The locus of the point of simultaneous extinction generally forms a curve called an isoclinic line.

Each of the component rays broken up in the specimen, changes its velocity of transmission according to the magnitude of the stress (or strain) which exists in the vibration direction of that ray. Hence a certain amount of phase difference is produced between the two after passing through the specimen. If a specimen is placed in the beam of circularly polarized monochromatic light between the nicols crossed, the intensity of light $I$ passing through the analyzer may be represented by an equation of the form, as is well-known,

$$I=A^2\sin^2\frac{1}{2}\delta$$

where $A$ is a constant depending on the nature of the light used and $\delta$ the phase difference between the two components. Now consider a point giving such a phase difference as $\delta=2n\pi$ where $n$ is an integer; then we have $I=0$ at the point, that is, the light is extinguished and the field becomes dark. This darkness, depending on the magnitude of the stress (or strain), we shall speak of as *the photo-elastic extinction of the second kind*, which occurs periodically as $\delta$ increases. Thus $n$ represents *the order of extinction*.

## 2. Relation between stress and optical effect.

According to the usual practice we take stress for the present as a basis of optical effect. Then the relation between stress and optical effect may be generally represented by either of the equations

$$\left.\begin{aligned} r&=CSd \\ \delta&=2\pi CSd/\lambda \end{aligned}\right\} \quad \cdots\cdots\cdots\cdots\cdots\cdots\cdots\cdots\cdots\cdots\cdots\cdots(1)$$

where $r$: the relative retardation corresponding to $\delta$ (phase difference at a point),

$S$: the principal stress difference,

$d$: the thickness of the specimen,

$C$: the photo-elastic (stress-optical) constant,

$\lambda$: the wave length of the light used.

In technical units, $C$ may be expressed as $\mathrm{cm^2\,kg^{-1}}$, as will be seen from (1). It will be more familiar to engineers to use another constant $K$ defined by the equation

$$K=2\pi Sd/\delta \quad \cdots\cdots\cdots\cdots\cdots\cdots\cdots\cdots\cdots\cdots\cdots\cdots\cdots\cdots\cdots\cdots\cdots\cdots(2)$$

the units of $K$ being kg/cm as shown below. Then at the point where $\delta=2n\pi$, we have

$$Sd=Kn \quad \ldots\ldots(3)$$

Thus at the point of the photo-elastic extinction of the second kind, *the principal stress difference multiplied by the thickness of the specimen is proportional to the order of extinction.* This relation we shall refer to as *the Law of Photo-elastic Extinction,* and the constant $K$ as *the Coefficient of Photo-elastic Extinction.* In a specimen of uniform thickness, the law may be expressed in another form, namely,

$$S=kn \quad \ldots\ldots(4)$$

where $k=K/d$. Hence *the principal stress difference is directly proportional to the order of extinction.* If $S$ is expressed in kg/cm$^2$ and $d$ in cm, then $K$ is measured in kg/cm and $k$ in kg/cm$^2$.

From the equations (1) and (2) we get the relation $KC=\lambda$. By L. N. G. FILON the constant $C$ is expressed in a unit called *a brewster*[1], which is defined as an *ångström* per millimetre per bar and is equal to [$10^{-13}$ cm$^2$ per dyne] or [980 cm$^2$/($10^{10}$ kg)]. Hence we have the relation

$$(K \text{ in kg/cm})\times(C \text{ in } brewsters)=(KC)\ \frac{\text{kg}}{\text{cm}}\ \frac{980\ \text{cm}^2}{10^{10}\ \text{kg}}$$
$$=9.8\,(KC)\ \mathring{a}ngstr\ddot{o}ms$$

This must be equal to $\lambda$. It $\lambda$ is expressed in *ångströms*, we have

$$(K \text{ in kg/cm})\times(C \text{ in } brewsters)=(\lambda \text{ in } \mathring{a}ngstr\ddot{o}ms)/9.8$$

The next step is to consider how to determine the value of *the coefficient* $K$. Let a BABINET'S compensator be inserted between crossed nicols in such a position that the principal planes of vibration of the former are inclined at 45° to the principal planes of the latter. The distance through which a wedge is moved in order to replace a dark band with an adjoining one we shall denote by $a$. In the compensator employed by the author, the distance $a$ was found equal to 3.82 mm for the green light ($\lambda=5\,461$ *ångströms*) of the mercury vapour lamp. The phase difference increased by the compensator displacement $a$ is equal to $2\pi$.

Next, if a tension or compression specimen of uniform section is inserted between the compensator and the polarizer arranged as before with the directions of principal stresses placed parallel to the principal planes of the compensator, we find the central band shifted to another position. A wedge is now to be moved by the micrometer screw until the central band comes again to the initial position. If this distance, *the band displacement,* is denoted by $x$, we have

$$\delta=2\pi x/a$$

where $\delta$ is the phase difference corresponding to the displacement $x$. Then we

(1) *Phil. Trans. A*, CCXXIII, p. 106 (1923).

obtain from this and the equation (2)

$$P = xKb/a \quad \ldots\ldots (5)$$

as $S = P/bd$ in a tension or compression specimen, $b$ being the width of the specimen and $P$ the axial load applied to the specimen.

If the photo-elastic behaviour of the specimen arranged as above is studied by increasing the load, measuring the corresponding band displacement, and plotting a curve with the loads as ordinates and the band displacements as abscissas, we get *a load-band displacement curve*. Since the tangent of the slope of *a load-band displacement curve* indicates the values of $Kb/a$ in (5), *the coefficient* $K$ is equal to the tangent value multiplied by a constant $a/b$.

### 3. Determination of the coefficient of photo-elastic extinction; Time effect.

Eleven tension specimens as shown in **Fig. 1** were first prepared in order to determine *the coefficient* $K$ for phenolite. The day before each testing, the specimen was annealed by heating it at 65° C. for about an hour in a thermostat and allowing it to cool off very slowly, the object being the removal of initial stress. A cement-briquette testing machine of MICHAELIS' type was used as the straining apparatus. The grips of the machine were modified to fit into the holes drilled at the two ends of the specimens to enable the pull to be applied. For light, the green line ($\lambda = 5\,461$ *ångströms*) of the mercury vapour lamp was used throughout the experiments. **Fig. 2** shows the general view of the apparatus, and **Fig. 3** the tension device in which the transparent specimen is photographed black, owing to the fact that phenolite, yellowish orange in colour, absorbs the light

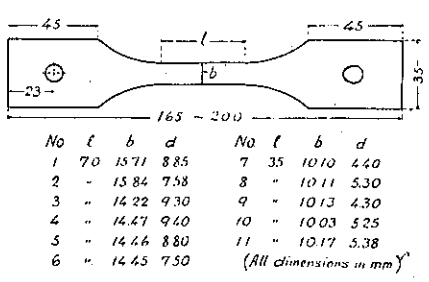


| No | $l$ | $b$ | $d$ | No | $l$ | $b$ | $d$ |
|---|---|---|---|---|---|---|---|
| 1 | 70 | 15.71 | 8.85 | 7 | 35 | 10.10 | 4.40 |
| 2 | " | 15.84 | 7.58 | 8 | " | 10.11 | 5.30 |
| 3 | " | 14.22 | 9.30 | 9 | " | 10.13 | 4.30 |
| 4 | " | 14.47 | 9.40 | 10 | " | 10.03 | 5.25 |
| 5 | " | 14.46 | 8.80 | 11 | " | 10.17 | 5.38 |
| 6 | " | 14.45 | 7.50 | (All dimensions in mm) | | | |

**Fig. 1.**

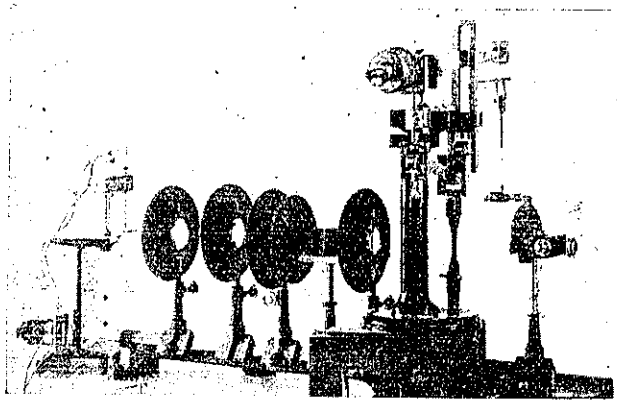

**Fig. 2.**

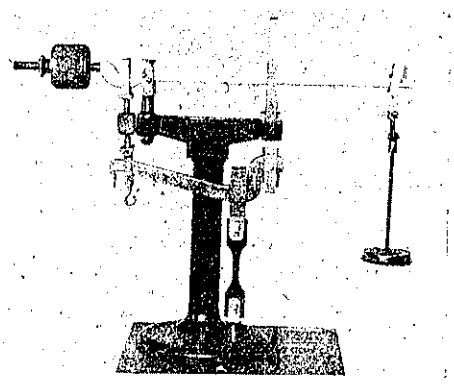

**Fig. 3.**

sensitive to the ordinary photographic plate.

It was attempted first to obtain *the load-band displacement curves* by increasing the load by $\Delta P$ kg at intervals of $\Delta t$ minutes, and measuring the band displacement at the instant 1 minute after each increase of load. Five series of tests were carried out by changing the load and time increments.

*The load-band displacement curves* proved linear, the value of $K$ being found as follows:—

| | | | | | |
|---|---|---|---|---|---|
| $\Delta P$, kg | 30 | 15 | 5 | 5 | 5 |
| $\Delta t$, min. | 2 | 2 | 2 | 5 | 10 |
| $K$, kg/cm | 10.9 | 10.3 | 9.9 | 9.6 | 8.9 |

These results indicate that the method of testing used above fails to give a constant value of $K$.

In the second attempt it was performed within five seconds to carry out the three operations of loading, reading the compensator, and unloading for a definite value of load. Such an observation was repeated at intervals of more than 5 minutes with the same specimen in order to avoid the effect of residual strain. The load was varied stepwise in several ways within the limits of 10 and 80 kg. *The load-band displacement curves* of eleven specimens were found linear within the limits of the load applied. In this case the coefficient seemed to be little affected by the history of loading. The values of $K$ determined by the method of least squares varied from 10.75 to 11.44 kg/cm in the eleven specimens. The mean value was 11.0 kg/cm.

For the purpose of compression tests, a steel frame was inserted between the grips of the testing machine to convert it into a compression tester, the device being shown in **Fig. 4.** In order to examine the very material used in the previous tests, nine specimens, 72 mm in length, were prepared by cutting off both ends of the tension specimens. Each specimen was tested by the instantaneous method as was applied in the tension tests. The load limits were 30 and 100 kg. The value of $K$ determined by the method of least squares varied from 10.66 to 11.53 kg/cm in the nine specimens, giving the mean value of 11.0 kg/cm.

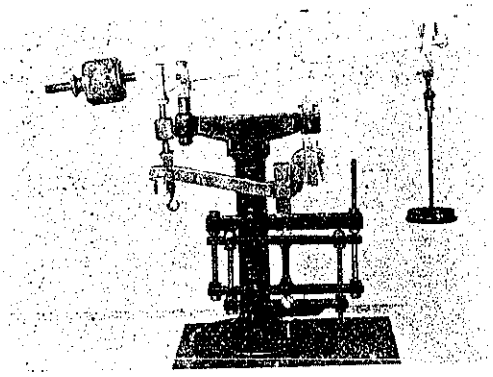

**Fig. 4.**

The value of the coefficient of photo-elastic extinction determined by the instantaneous method as was applied in the above tests we shall refer to as *the pri-*

*mitive value of* $K$, and denote it by $K_0$.

The equation (5) can be transformed into

$$Sad=xK$$

in which the left- and right-hand members must be respectively constant so long as the stress remains constant, while $x$ may undergo a change in consequence of the optical creep. Hence $K$ may be a function of time to neutralize the variation of $x$. The stress-optical condition at the instant of loading will be now denoted by

$$Sad=x_0K_0$$

and the condition at $t$ minutes after loading by

$$Sad=(x_0+X)K_t$$

where $X=x-x_0$. Eliminating $x_0$ from those two relations, we have

$$K_t=K_0(1+K_0Y/S)^{-1} \quad \cdots\cdots(6)$$

where $Y=X/ad$, representing the optical creep per unit thickness expressed in multiple of the unit defined by the distance $a$.

In order to determine the value of $Y$, eleven tension specimens of phenolite were examined under various stresses (10~230 kg/cm$^2$). Each test was performed by keeping the load constant and observing the band displacement $X$ at intervals of 1 minute for the first 20 minutes and then at intervals of 10 minutes for the following 100 minutes. It took a few months to carry out the above experiments, so the room temperature varied from 14° to 21° C. On calculating $Y$ and plotting it to time on the logarithmic paper, we find that *the creep-time relation* can be represented by equations of the form

$$Y=pt^r$$

The results of more than sixty tests showed that the ratio of $Y/S$ for a definite value of $t$ is nearly a constant, as can be seen from the following table in which eleven series of the results are given as typical cases. Thus we take $p$ to be proportional to $S$, and we have

**Table of $Y/S$ in $10^{-4}$ cm per kg.**

| $t$ min. | $Y/s$ observed under the stress in kg/cm$^2$ | | | | | | | | | | | mean $Y/s$ obs. | $Y/s$ cal. | Diff. |
|---|---|---|---|---|---|---|---|---|---|---|---|---|---|---|
| | 20 | 40 | 60 | 80 | 100 | 120 | 130 | 160 | 180 | 200 | 220 | | | |
| 1 | 35 | 33 | 30 | 32 | 31 | 34 | 34 | 33 | 32 | 34 | 31 | 33 | 33 | 0 |
| 2 | 45 | 41 | 40 | 44 | 42 | 43 | 44 | 42 | 43 | 44 | 42 | 43 | 43 | 0 |
| 3 | 50 | 48 | 47 | 50 | 50 | 50 | 49 | 49 | 50 | 53 | 49 | 50 | 50 | 0 |
| 5 | 60 | 55 | 57 | 62 | 60 | 58 | 60 | 59 | 60 | 63 | 59 | 59 | 60 | 1 |
| 10 | 75 | 70 | 73 | 79 | 78 | 73 | 78 | 76 | 76 | 78 | 74 | 76 | 76 | 0 |
| 15 | 85 | 83 | 85 | 90 | 88 | 81 | 87 | 86 | 87 | 90 | 85 | 86 | 88 | 2 |
| 20 | 95 | 93 | 93 | 98 | 95 | 91 | 96 | 93 | 96 | 98 | 96 | 95 | 96 | 1 |
| 30 | 105 | 103 | 104 | 114 | 105 | 103 | 108 | 105 | 102 | 110 | 107 | 106 | 107 | 1 |
| 60 | 125 | 125 | 125 | 141 | 125 | 128 | 135 | 128 | 129 | 135 | 136 | 130 | 131 | 1 |
| 90 | 135 | 145 | 140 | 160 | 140 | 144 | 156 | 150 | 142 | 152 | 150 | 147 | 148 | 1 |
| 120 | 145 | 155 | 148 | 169 | 152 | 161 | 171 | 167 | 150 | 165 | 166 | 159 | 160 | 1 |

$$\left.\begin{aligned} Y&=\frac{1}{300}St^{0.36} \quad (t<15\text{ min.}) \\ Y&=\frac{1}{250}St^{0.29} \quad (15\text{ min.}<t<120\text{ min.}) \end{aligned}\right\} \quad \cdots\cdots(7)$$

The accuracy of these equations may be judged from the table, which gives also the calculated values of $Y/S$ and the difference between the observation and the calculation.

If we insert (7) into (6), we have

$$K_t = K_0(1+mK_0t^r)^{-1} \quad \ldots\ldots(8)$$

where $m$ represents the numerical coefficients and $r$ the indices in the expression (7). Taking $K_0$ at 11.0 kg/cm, we have the values of $K_t$ from the equation (8) as follows :—

$K_1 = 10.6$ $K_2 = 10.5$ $K_5 = 10.3$
$K_{15} = 10.0$ $K_{30} = 9.8$ $K_{120} = 9.4$

Accordingly it is obvious that the isochromatic lines observed in the experiment vary with time by the optical creep.

## 4. Comparison of phenolite with glass, celluloid and bakelite.

**(1)** Just in the same way as for phenolite, the values of $K_0$ for some other materials were obtained as follows :—

| Materials | Glass | Celluloid | Bakelite | Phenolite |
|---|---|---|---|---|
| $K_0$, kg/cm | 234.4 | 48.8 | 12.7 | 11.0 |
| $C$, *brewsters* | 2.4 | 11.4 | 43.9 | 50.6 |

Three specimens made of so-called Belgian polished glass were tested. Celluloid specimens, twelve in all, were cut from the sheets manufactured by *the Dainippon Celluloid Co.*, Japan, *the Du Pont Viscoloid Co.*, U. S. A., and *the British Xylonite Co.*, London. Three bakelite specimens were prepared out of the pure bakelite of $C$ state supplied by *the Sankyo Co.*, Tokyo.

The above table shows that the value of $K_0$ of celluloid is nearly five times as large as that of phenolite. This is in agreement with Tuzi's result obtained by a different method.[1] Among these substances, glass gives the largest value of $K_0$. In this respect it is not suitable for the photo-elastic experiment.

**(2)** Phenolite has considerable initial stress in it. But it can be removed by one hour's annealing at 65° C. On the other hand, initial stress in bakelite is so marked and stubborn that it can not be easily removed as in phenolite. In this point bakelite compares unfavourably with phenolite.

**(3)** The value of stress corresponding to the end of linearity in *the load-band displacement curve* we shall speak of as the optically proportional limit, and denote it by $S_0$. A number of tests for phenolite showed that it was equal to about 280 kg/cm$^2$ for tension and 300 kg/cm$^2$ for compression. The law of photo-elastic ex-

(1) *Sci. Pap. I. P. C. R.*, VI, p. 79 (1927).

tinction holds true only below $S_0$. Hence there is a certain limit in the order of extinction for a given value of the thickness $d$. Denoting it by $n_0$, we have the relation

$$n_0 = S_0 d / K_0$$

The mean value of $S_0$ for celluloid was found to be about 190 kg/cm$^2$ with the specimens described in (1), while that given by COKER and CHAKKO[1] is about 250 kg/cm$^2$. Taking the latter value for the comparison with phenolite, we get the following values of $n_0$, the value of $S_0$ for phenolite being taken at 280 kg/cm$^2$.

| | | | |
|---|---|---|---|
| $d$ in cm | 1.0 | 0.6 | 0.4 |
| $n_0$ for phenolite | 25.4 | 15.3 | 10.2 |
| $n_0$ for celluloid | 5.1 | 3.1 | 2.1 |

Thus the value of $n_0$ for celluloid is one-fifth of that for phenolite. In this point celluloid compares unfavourably with phenolite.

(4) The average values of some physical constants obtained from several specimens are as follows:—

| Materials | Phenolite | Bakelite | Celluloid |
|---|---|---|---|
| Coef. of linear expansion C., $10^{-5}$ | 7 | 9 | 11 |
| Ultimate tensile strength, kg/cm$^2$ | 430 | 250 | 430 |
| Ultimate compressive strength, kg/cm$^2$ | 1 600 | 1 100 | 1 200 |
| Yield point (compression), kg/cm$^2$ | 1 600 | 1 000 | 540 |
| Young's modulus, kg/cm$^2$ $10^4$ | 3.6 | 3.7 | 2.7 |

The coefficient of linear expansion was determined for the temperature range 5°~50° C with the LEMEN and WERNER's apparatus supplied by *Goerz Werk*. The YOUNG's modulus varies according to the mode of testing. The values given in the table are the results obtained by loading the specimen in a moderate rate without interruption. By loading and unloading very quickly as in the method applied to the determination of the coefficient $K$, the value for phenolite was found to be $4.3 \times 10^4$ kg/cm$^2$.

## 5. Procedure of the photo-elastic observation.

In the engineering application of photo-elasticity the optical effect is remarkably affected by the time elapsed after loading. In the absence of care, this may give rise to an error in interpreting the isochromatic lines. To avoid this source of error the following procedure is recommended.

(1) **Isochromatic lines.** The specimen placed in the beam of circularly polarized monochromatic light should be photographed at an instant $t$ minutes after

(1) *Phil. Trans. A*, CCXXI, p. 139 (1921).

loading. To make the order of extinction be correctly judged, photographs should be taken, if necessary, at various stages of loading.

(2) **Sign of the principal stress difference.** This may be discriminated with ease if a few points on the specimen are examined with a comparison test piece, of which the material and the thickness need not be the same as those of the specimen.

(3) **Isoclinic lines.** They should be then recorded successively. If there is the creep in this case too, each line should be photographed at the instant $t$ minutes after loading in order to avoid the effect of residual strain.

(4) **Coefficient $K_t$.** The value of the coefficient $K_t$ should be determined for the same material as that of the specimen, and then $k_t=K_t/d$ be calculated. The value of the principal stress difference for the dark bands photographed should be estimated by the relation $S=nk_t$.

(5) **Principal stresses.** The principal stress should be determined by the method of graphical integration[1]. The method of measuring the sum of the principal stresses at several points of a specimen seems to be incorrect, as it may give rise to an error due to the creep of strain.

## Chapter 2. Relation between Strain and Optical Effect.

### 6. Further study of time effect.

As explained in Chapter 1 the stress-optical effect at the instant $t$ minutes after loading may be denoted by the expression

$$Sad=(x_0+X)K_t$$

In order to compare the strain with the optical effect, the total optical effect $(x_0+X)$ is now considered, as the strain is measured without separating it into the initial value and the creep. By doing so we obtain a general view of the optical effect varying with the time, though the accuracy is not so good as in the preceding chapter. Now we put

$$y=S/K_t=(x_0+X)/ad$$

Then the quantity $y$ represents the total optical effect per unit thickness at any instant in a similar way to $Y$ in the equation (6) of Chapter 1.

From the data obtained in the experiments explained in Chapter 1, the values of $y$ were calculated, and they were plotted to time on the logarithmic paper. The curve drawn through the points belonging to a definite value of the stress $S$ was found linear. Accordingly it may be represented by the equation of the form

(1) *British Association Report*, 1914, p. 201 and 1923, p. 350.

$$y=\beta S t^{r}$$

The coefficient $\beta$ and the index $r$ for $t<16$ minutes were found as follows:—

$$\beta=0.0939\pm0.00005$$
$$r=0.0271\pm0.0002$$

Hence we have

$$y=0.0939\ S t^{0.0271}$$

This relation holds good for any value of $t$ between $t=1$ minute and $t=16$ minutes.

## 7. Strain measurement.

The tension apparatus and the tension specimens that were employed in the optical measurements were again used for observing the strain. The elongations on the gauge length of 20 mm were measured by HUGGENBERGER'S tensometer, of which one division of the scale corresponds to 1/1 200 mm. A number of tests were carried out under various loads. Each set of observations was performed by keeping the load constant and taking the reading of the tensometer at intervals of 1 minute for the first 16 minutes. The room temperature during the period of these tests varied from 13° to 18° C. Since the size of the phenolite plates supplied was comparatively small, the tension specimens with relatively long gauge length could not be prepared. This restriction of the gauge length limited the measurement to the first 16 minutes, as the creep for the following 20~120 minutes was relatively small and it seemed very difficult to measure it with precision.

The tensometer readings for each set of observations were plotted to time on the logarithmic paper. It was then found that the strain-time relation can be represented by the equation of the form

$$\varepsilon=\beta' S t^{z}$$

where $\varepsilon$ is the strain, $S$ the stress in kg/cm$^2$ and $t$ in minutes. The coefficient $\beta'$ and the index $z$ were found as follows:—

$$\beta'=(0.2338\pm0.0002)\times10^{-4}$$
$$z=\ 0.0288\pm0.0002$$

Hence we get for phenolite

$$\varepsilon=0.2338\times10^{-4}\ S t^{0.0288}$$

## 8. Strain and optical effect.

In the above two articles it was found that the optical effect and also the strain undergo the time effect; namely,

$$y=0.0939\ S t^{0.0271}$$
$$\varepsilon=0.2338\times10^{-4}\ S t^{0.0288}$$

The rate of change of $y$ with the time differs slightly from that of $\varepsilon$. The

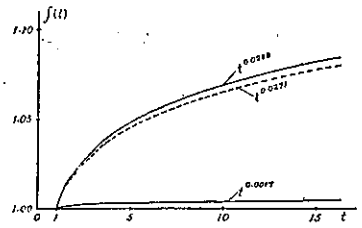


Fig. 5.

difference of the two indices is

$$0.0288-0.0271=0.0017$$

The values of $t^{0.0288}$, $t^{0.0271}$ and $t^{0.0017}$ are plotted in **Fig. 5.** If we eliminate the stress $S$ from the above two equations, we get

$$y=K'\varepsilon$$

where

$$K'=\frac{0.0939}{0.2338}\times 10^4\, t^{-0.0017}=4\,020\, t^{-0.0017}$$

The coefficient $K'$ calculated for some values of $t$ are shown in the next table, in which the value of $t^{0.0017}$ are also given.

| $t$ | 1 | 2 | 5 | 10 | 15 |
|---|---|---|---|---|---|
| $K'$ | 4 020 | 4 015 | 4 009 | 4 004 | 4 002 |
| $t^{0.0017}$ | 1.0000 | 1.0012 | 1.0027 | 1.0039 | 1.0046 |

Now it is apparent that if we neglect some errors less than 0.5 %, the coefficient $K'$ may be considered approximately as a constant. We are thus driven to the conclusion that the strain may be the immediate factor in producing the photo-elastic phenomenon, so far as the above experiments are concerned.

## 9. Discussion of the result.

### (a) Lateral strain.

There is still a question whether the lateral strain takes part in producing the double refraction. In order to investigate this problem, a number of tension tests were made to measure the lateral strain under various loads. The apparatus described above was again used. Two specimens of phenolite were prepared for the present purpose. The shape of the specimens was nearly the same as those used before, except that the width was 25 mm at the centre and 50 mm at the ends. Each set of observations was carried out by keeping the load constant, and reading the lateral contraction at intervals of 1 minute for the first 16 minutes. The room temperature during this period varied from 13° to 18° C.

Plotting the observed values of the lateral contraction to time on the logarithmic paper, it was found that the strain-time relation can be represented by the equation of the form

$$\varepsilon'=\beta'' S t^w$$

where $\varepsilon'$ is the lateral strain. It was found that the coefficient $\beta''$ and the index $w$ are as follows;

$$\beta''=(0.0833\pm 0.00009)\times 10^{-4}$$
$$w = 0.0287\pm 0.0002$$

Hence the lateral strain $\varepsilon'$ is given by

$$\varepsilon' = 0.0833 \times 10^{-4}\, S\, t^{0.0287}$$

As the longitudinal strain is given by the equation

$$\varepsilon = 0.2338 \times 10^{-4}\, S t^{0.0283}$$

the value of Poisson's ratio of phenolite is

$$1/m = \varepsilon'/\varepsilon = 0.356\, t^{-0.0001}$$

The index of $t$ in this expression being smaller than the corresponding probable error in magnitude, it may be said that Poisson's ratio of phenolite undergoes little time effect. We have therefore

$$1/m = 0.356 \quad \text{or} \quad m = 2.81$$

Hence the lateral strain $\varepsilon'$ can be represented by means of the relation

$$\varepsilon' = -\varepsilon/m$$

Take for the present the greatest shearing strain $\gamma$ as the immediate cause of the optical effect instead of the linear strain taken in the previous article. Then introducing a constant $K''$, we may put

$$y = K'' \gamma$$

From the mathematical theory of elasticity it is known that the principal strain difference $(\varepsilon - \varepsilon')$ at a point is equal in magnitude to the greatest shearing strain at the point. Hence we have

$$y = K'' (\varepsilon - \varepsilon').$$

This gives

$$y = \frac{m+1}{m} K'' \varepsilon .$$

As $m$ is practically independent of the time effect, the coefficient $K''$ varies with time in a similar way to $K'$ in the equation

$$y = K' \varepsilon$$

Thus the consideration of the lateral strain adds nothing new to the interpretation of creep in the case of phenolite.

### (b) Other materials than phenolite.

As to the relation between strain and optical effect, a number of experiments have been made by various authors with specimens of glass, celluloid and bakelite. As for glass, Filon and Jessop[1] tested a number of rectangular blocks of glass with the result that there was neither optical creep during the time the load was left on, nor any trace of residual double refraction on removal of the load. In their tests the blocks were left under the compressive stress of 149～220 kg/cm$^2$ for 17～67 hours.

S. R. Savur[2] showed with specimens of glass that the dark band took its final

(1) *Phil. Trans. A.*, ccxxiii, p. 91 (1923).
(2) *Phil. Mag.*, l, p. 459 (1925).

position simultaneously with the application of the load and that no residual effect could not be observed when the load was removed.

The result obtained by K. OKUDA[1] with a tension specimen of glass, which was left under the stress of 400 kg/cm$^2$ for 17 hours at the room temperature, showed that no residual double refraction was detected in it after the removal of the stress.

As for celluloid, there have been also some investigations[2]. Experiments carried out by FILON and JESSOP with tension specimens indicated that the optical retardation shows an immediate effect on loading, very nearly proportional to the applied load, followed by a progressive creep until an equilibrium value is approached, and that the strain follows the laws closely similar to those of the optical retardation, the initial value being also approximately proportional to the applied load. According to their result, the retardation $r$ and the strain $\varepsilon$ are connected with the time $t$ by the relations

$$r=r_0+pt^{1/3}+qt$$
$$\varepsilon=\varepsilon_0+at^{1/3}+bt$$

where the constants $r_0$ and $\varepsilon_0$ are proportional to the applied stress $T$, $p$ and $a$ are very roughly proportional to $T^2$, and $q$ and $b$ are small and irregular. On examining the relation between strain and optical effect, the result they obtained does not conform to the hypothesis that stress is the immediate factor in producing artificial double refraction, and also the hypothesis which makes strain the essential factor. Thus they were led to establish the linear law

$$r=\alpha T+\beta\varepsilon$$

where the constants $\alpha$, $\beta$ are found to vary within fairly narrow limits for any given specimen. They have also shown that COKER and CHAKKO's result may be expressed by the relation

$$r=a+bT+c\varepsilon$$

where the first term on the right shows the initial stress and optical effect existing in the material before loading. Hence it appears that the result COKER and CHAKKO is in agreement with that of FILON and JESSOP.

As for bakelite, no particular observations seem ever to have been made except the experiments carried out by I. ARAKAWA[3], who measured the optical effect with specimens of bakelite and not the strain. The result of his observations showed that the formula

$$r=r_0+pt^{1/3}+qt$$

(1) *Memoirs Coll. Eng. Kyushu Imp. Univ.*, III, p. 172 (1927).

(2) FILON and JESSOP, *loc. cit.*; COKER and CHAKKO, *Phil. Trans. A.*, CCXXI, p. 149 (1921); RAMSPECK, *Ann. der Physik*, LXXIV, p. 722 (1924).

(3) *Proc. Phys. Math. Soc. Japan*, V, p. 117 (1923).

also holds good in the case of bakelite, the constants $\tau_0$ and $p$ being roughly proportional to the stress $T$, and $q$ small.

Now it is worthy of remark that the constant $p$ is roughly proportional to $T$ in bakelite and to $T^2$ in celluloid. As the creep-time relation for phenolite is represented by the equation of the form $Y=pt^n$ where $p$ is proportional to the stress, it appears that the stress-optical property of phenolite is very near to that of bakelite. This may be due to the fact that phenolite and bakelite are chiefly made of the same materials, i.e. formaldehyde and phenol.

### (c) Temperature effect.

The measurements of strain and optical effect described above were carried out in a few months, so the room temperature varied from 13° to 21° C. In each series of optical tests which continued some 2 hours, the temperature varied within 2°, while the temperature remained nearly constant during each set of the strain measurements which continued some 20 minutes. In the temperature range above mentioned, the effect of temperature on the optical phenomenon is not clear, but it is likely that this source of effect may exist. In this respect, further investigations are needed by taking a wider range of temperature, say 30° C. or more.

## PART II.
## STRESS DISTRIBUTION IN SOME TWO-DIMENSIONAL PROBLEMS.

### Chapter 3. Roller Diametrically Compressed.

### 10. Solution of the problem.

A number of mathematical solutions and photo-elastic experiments have been carried out for a roller diametrically compressed[1]. In this chapter the same problem is taken up to show that the method proposed by Prof. S. YOKOTA[2] can be conveniently applied to such a problem. In this method stress-components are given by two general equations, which contain two arbitrary functions of complex variables and the first derivative of one of them. In solving a problem the arbitrary functions should be properly chosen with due attention to the boundary conditions.

Prof. YOKOTA's general expression for stress-components in two-dimensional

(1) HERTZ, *Ges. Werk*, I, p. 285; MICHELL, *Proc. London Math. Soc.*, XXXII, p. 35 (1900); MESNAGER *Ann. P. et Ch. Mém.*, (71) IV, p. 160 (1901); HUBER and FUCHS, *Phys. ZS.*, XV, p. 298 (1914); KÖNIG, *Ann. der Phys.*, (4) LII, p. 553 (1917); STEINHEIL, *Diss. Giesen*, (1920); FILON, *Brit. Ass. Rep.* Liverpool, p. 354 (1923); FÖPPL, *Drang und Zwang*, I, p. 320 (1924); ARAKAWA, *loc. cit.*; RIETH, *Ann. der Phys.*, (4) LXXIX, p. 145 (1926).

(2) *Jour. Soc. Mech. Eng.* (Japan), XVIII, April 1915.

problems of elasticity, referred to a system of rectangular coordinates $z=x+iy$, is represented by a pair of equations of the form

$$\sigma_x-\sigma_y-2i\tau=2iyF_1'(z)+F_2(z)$$
$$\sigma_x+\sigma_y=2R[F_1(z)]$$

where $F_1(z)$ and $F_2(z)$ are arbitrary functions of $z$, and $R[F_1(z)]$ represents the real part of the function $F_1(z)$. The stress-components referred to a system of curvilinear orthogonal coordinates $(\alpha,\beta)$ are shown to be connected with these written above by the equations

$$\widehat{\alpha\alpha}-\widehat{\beta\beta}-2i\widehat{\alpha\beta}=e^{2i\gamma}\{\sigma_x-\sigma_y-2i\tau\}$$
$$\widehat{\alpha\alpha}+\widehat{\beta\beta}=\sigma_x+\sigma_y$$

where $\gamma$ is the angle which the external normal to a curve of the $\alpha$-family makes with the positive axis of $x$.

Now we may take a system of coordinates $(\alpha,\beta)$ defined by the equation

$$z=ae^{-w} \qquad \cdots\cdots(1)$$

where $z=x+iy,\quad w=\alpha+i\beta$

$$\alpha\geqq 0,\quad \beta^2\leqq\pi^2$$

In the case when $\alpha=0$, the equation gives the circumference of a circle with radius $a$, the centre being given by $\alpha=\infty$ as shown in **Fig. 6.** In this system of coordinates, the curves of the $\alpha$-family on the $z$-plane are concentric circles with the centre at the origin of that plane, and the corresponding curves of the $\beta$-family are straight lines radiating from the origin. In the equation (1) the coordinate $\beta$ is the angle which the radius vector makes with the positive axis of $x$, and it is negative when the radius vector rotates counter-clockwise. Thus the external normal at a point to the $\alpha$-curve is coincident with the $\beta$-curve, the radius vector, passing through the point under consideration, and the normal makes an angle $(-\beta)$ with the positive axis of $x$.

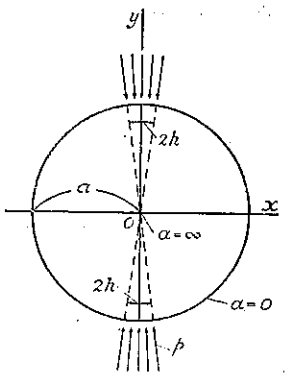

Fig. 6.

Hence we have $\gamma=-\beta$. Therefore we get

$$\left.\begin{aligned}\widehat{\alpha\alpha}-\widehat{\beta\beta}-2i\widehat{\alpha\beta}&=e^{-2i\beta}[2iyF_1'(z)+F_2(z)]\\ \widehat{\alpha\alpha}+\widehat{\beta\beta}&=2R[F_1(z)]\end{aligned}\right\} \qquad \cdots\cdots(2)$$

From the equation (1) we have

$$y=-ae^{-\alpha}\sin\beta$$

Inserting this into the first equation of (2), we get

$$\begin{aligned}\widehat{\alpha\alpha}-\widehat{\beta\beta}-2i\widehat{\alpha\beta}&=e^{-2i\beta}[-2iae^{-\alpha}\sin\beta F_1'(z)+F_2(z)]\\ &=-e^{-2i\beta}[ae^{-\alpha}(e^{i\beta}-e^{-i\beta})F_1'(z)-F_2(z)]\\ &=(1-e^{-2i\beta})(-ae^{-w})F_1'(z)-e^{\alpha-i\beta}(-e^{-w})F_2(z)\end{aligned}$$

On changing the independent variables from $z$ to $w$, we put

$$f_1(w)=F_1(z)$$
$$f_2(w)=-e^{-w}F_2(z)$$

Then

$$f_1'(w)=F_1'(z)\frac{dz}{dw}=-ae^{-w}F_1'(z)$$

Hence the expression (2) is written as

$$\left.\begin{aligned}&\widehat{\alpha\alpha}-\widehat{\beta\beta}-2i\widehat{\alpha\beta}=(1-e^{-2\beta})f_1'(w)-e^{\alpha-i\beta}f_2(w)\\&\widehat{\alpha\alpha}+\widehat{\beta\beta}=2R[f_1(w)]\end{aligned}\right\}\quad\cdots\cdots(3)$$

This is the general expression for stress-components in the case where the orthogonal coordinates defined by (1) are used. This form is convenient in treating the problem, as the boundary of the roller is given by the curve $\alpha=0$.

Let the load $P$ be distributed on the area $2hab$ with the uniform radial intensity $p$, where $b$ is the length of the roller and $2h$ the small angle made by the loaded arc as shown in **Fig. 6.** Then the boundary conditions in the first quadrant are

$$[\widehat{\alpha\beta}]_{\alpha=0}=0$$
$$[\widehat{\alpha\alpha}]_{\alpha=0}=0 \quad \text{for} \quad (-\beta)<(\pi/2-h)$$
$$[\widehat{\alpha\alpha}]_{\alpha=0}=-p \quad \text{for} \quad (-\beta)>(\pi/2-h)$$

The conditions for $\widehat{\alpha\alpha}$ may be expressed in an equation of the form

$$[\widehat{\alpha\alpha}]_{\alpha=0}=-\frac{2p}{\pi}\left[h+\sum_{n=1}^{\infty}(-1)^n\frac{1}{n}\sin 2nh\cos 2n\beta\right]\quad\cdots\cdots(4)$$

which holds for $0\leqq|\beta|\leqq\pi$. The boundary conditions in the other three quadrants are naturally fulfilled from symmetry.

Now we put

$$f_1(w)=\frac{2p}{\pi}\sum_{n=0}^{\infty}A_{2n}e^{-2nw}$$

$$f_2(w)=\frac{2p}{\pi}\sum_{n=0}^{\infty}B_{2n+1}e^{-(2n+1)w}$$

Inserting these relations into the first equation of (3), we have

$$\widehat{\alpha\alpha}-\widehat{\beta\beta}-2i\widehat{\alpha\beta}=-\frac{2p}{\pi}\left[(1-e^{-2i\beta})\sum_{n=0}^{\infty}2nA_{2n}e^{-2nw}+e^{\alpha-i\beta}\sum_{n=0}^{\infty}B_{2n+1}e^{-(2n+1)w}\right]$$

This may be written after rearrangement

$$\widehat{\alpha\alpha}-\widehat{\beta\beta}-2i\widehat{\alpha\beta}$$
$$=-\frac{2p}{\pi}\sum_{n=0}^{\infty}e^{-2n\alpha}\left\{2(n+1)A_{2(n+1)}e^{-2\alpha}+B_{2n+1}-2nA_{2n}\right\}e^{-2(n+1)i\beta}\quad\cdots\cdots(5)$$

Moreover from the second equation of (3) we have

$$\widehat{\alpha\alpha}+\widehat{\beta\beta}=\frac{2p}{\pi}\left[2A_0+2\sum_{n=1}^{\infty}A_{2n}e^{-2n\alpha}\cos 2n\beta\right]\quad\cdots\cdots(6)$$

If the two equations (5) and (6) are added together side by side, we have an equation which does not involve the term of the normal stress $\widehat{\beta\beta}$, namely,

$$\frac{\pi}{2p}\left[\widehat{\alpha\alpha}-i\widehat{\alpha\beta}\right]=\left\{A_0+\sum_{n=1}^{\infty}A_{2n}\,e^{-2n\alpha}\cos 2n\beta\right\}$$
$$-\frac{1}{2}\sum_{n=0}^{\infty}e^{-2n\alpha}\left\{2(n+1)A_{2(n+1)}e^{-2\alpha}+B_{2n+1}-2nA_{2n}\right\}e^{-2(n+1)i\beta}\quad\cdots\cdots(7)$$

As the shearing stress $\widehat{\alpha\beta}$ vanishes on the boundary, the imaginary part of the right-hand member of (7) must be zero when $\alpha=0$. Thus we have to put

$$2(n+1)A_{2(n+1)}+B_{2n+1}-2nA_{2n}=0$$

or
$$\{B_{2n+1}-2nA_{2n}\}=-2(n+1)A_{2(n+1)}\quad\cdots\cdots(8)$$

Then the remaining part of the equation (7) becomes, when $\alpha=0$,

$$\frac{\pi}{2p}\left[\widehat{\alpha\alpha}\right]_{\alpha=1}=A_0+\sum_{n=1}^{\infty}A_{2n}\cos 2n\beta\,.$$

Inserting the expression (4) into the left-hand member of this equation, we have

$$-\left\{h+\sum_{n=1}^{\infty}(-1)^n\frac{1}{n}\sin 2nh\cos 2n\beta\right\}=A_0+\sum_{n=1}^{\infty}A_{2n}\cos 2n\beta$$

In order that this relation holds, we take

$$A_0=-h\quad\cdots\cdots(9)$$

$$A_{2n}=(-1)^{n+1}\frac{1}{n}\sin 2nh\qquad(n\neq 0)\quad\cdots\cdots(10)$$

By introducing (8) and (10) in the equation (5), we obtain after calculation

$$\widehat{\alpha\alpha}-\widehat{\beta\beta}-2i\widehat{\alpha\beta}=-\frac{4p}{\pi}(e^{2\alpha}-1)\sum_{n=1}^{\infty}(-1)^n\sin 2nh\,e^{-2nw}\quad\cdots\cdots(11)$$

Again introducing (9) and (10) in (6), we get

$$\widehat{\alpha\alpha}+\widehat{\beta\beta}=-\frac{4p}{\pi}\left[h+\sum_{n=1}^{\infty}(-1)^n\frac{1}{n}\sin 2nh\cos 2n\beta\,e^{-2n\alpha}\right]\quad\cdots\cdots(12)$$

These equations enable us to calculate the stress-components at any point. If we put $\alpha=0$ in (11) and (12), we have

$$\widehat{\alpha\beta}=0$$
$$\widehat{\alpha\alpha}=\widehat{\beta\beta}$$
$$=-\frac{2p}{\pi}\left[h+\sum_{n=1}^{\infty}(-1)^n\frac{1}{n}\sin 2nh\cos 2n\beta\right]$$

which are the stresses on the boundary and are in accord with the boundary conditions.

In the inner domain excepting the circumference, the terms containing the infinite series may be replaced with simple expressions. Putting, for the sake of brevity,

$$\lambda_1=-e^{-2w+2ih},\quad\lambda_2=-e^{-2w-2ih},$$

we have, when $\alpha>0$,

$$|\lambda_1|<1, \quad |\lambda_2|<1$$

Then after long calculation here omitted we obtain

$$\sum_{n=1}^{\infty}(-1)^n \sin 2nh\, e^{-2nw}=\frac{1}{2i}\sum_{n=1}^{\infty}\left\{\lambda_1{}^n-\lambda_2{}^n\right\}$$

$$=\frac{1}{2i}\left[\frac{\lambda_1}{1-\lambda_1}-\frac{\lambda_2}{1-\lambda_2}\right]$$

$$=\frac{-e^{-2w}\sin 2h}{(1-\lambda_1)(1-\lambda_2)}$$

or

$$\sum_{n=1}^{\infty}(-1)^n \sin 2nh\, e^{-2nw}=-\frac{1}{D}e^{-2\alpha}\sin 2h\Big[(1+e^{-4\alpha})\cos 2\beta$$

$$+2e^{-2\alpha}\cos 2h-i(1-i^{-4\alpha})\sin 2\beta\Big] \quad \ldots\ldots\ldots\ldots\ldots\ldots\ldots\ldots\ldots\ldots(13)$$

where

$$D=\{1+e^{-4\alpha}+2e^{-2\alpha}\cos 2h\cos 2\beta\}^2-\{2e^{-2\alpha}\sin 2h\sin 2\beta\}^2$$

In regard to the equation (12), we obtain

$$\sum_{n=1}^{\infty}(-1)^n\frac{1}{n}\sin 2nh\cos 2n\beta\, e^{-2n\alpha}$$

$$=-\frac{1}{4i}\sum_{n=1}^{\infty}(-1)^{n-1}\frac{1}{n}e^{-2n\alpha}\left\{e^{2ni(h+\beta)}-e^{-2ni(h+\beta)}+e^{2ni(h-\beta)}-e^{-2ni(h-\beta)}\right\}$$

$$=-\frac{1}{4i}\Big[\log\{1+e^{-2\alpha+2i(h+\beta)}\}-\log\{1+e^{-2\alpha-2i(h+\beta)}\}$$

$$+\log\{1+e^{-2\alpha+2i(h-\beta)}\}-\log\{1+e^{-2\alpha-2i(h-\beta)}\}\Big]$$

Making use of the four equations of the type

$$\log\{1+e^{-2\alpha+2i(h+\beta)}\}=\log_e\Big[\{1+e^{-2\alpha}\cos 2(h+\beta)\}^2$$

$$+\{e^{-2\alpha}\sin 2(h+\beta)\}^2\Big]^{1/2}+i\,\mathrm{tg}^{-1}\frac{e^{-2\alpha}\sin 2(h+\beta)}{1+e^{-2\alpha}\cos 2(h+\beta)}$$

we obtain

$$\sum_{n=1}^{\infty}(-1)^n\frac{1}{n}\sin 2nh\cos 2n\beta\, e^{-2n\alpha}$$

$$=-\frac{1}{2}\Big[\mathrm{tg}^{-1}\frac{\sin 2(h+\beta)}{e^{2\alpha}+\cos 2(h+\beta)}+\mathrm{tg}^{-1}\frac{\sin 2(h-\beta)}{e^{2\alpha}+\cos 2(h-\beta)}\Big] \quad \ldots\ldots\ldots\ldots\ldots\ldots\ldots\ldots(14)$$

Inserting (13) into (11) and (14) into (12) respectively, we have

$$\left.\begin{aligned}\widehat{\alpha\alpha}-\widehat{\beta\beta}-2i\widehat{\alpha\beta}&=\frac{4p}{\pi D}(1-e^{-2\alpha})\sin 2h\Big[(1+e^{-4\alpha})\cos 2\beta\\&\quad+2e^{-2\alpha}\cos 2h-i(1-e^{-4\alpha})\sin 2\beta\Big]\\ \widehat{\alpha\alpha}+\widehat{\beta\beta}&=\frac{2p}{\pi}\Big[\mathrm{tg}^{-1}\frac{\sin 2(h+\beta)}{e^{2\alpha}+\cos 2(h+\beta)}+\mathrm{tg}^{-1}\frac{\sin 2(h-\beta)}{e^{2\alpha}+\cos 2(h-\beta)}-2h\Big]\end{aligned}\right\} \quad \ldots\ldots\ldots\ldots(15)$$

The first equation of (15) gives rise to the following two equations:—

$$\left.\begin{aligned}\widehat{\alpha\alpha}-\widehat{\beta\beta}&=\frac{4p}{\pi D}(1-e^{-2\alpha})\sin 2h\{(1+e^{-4\alpha})\cos 2\beta+2e^{-2\alpha}\cos 2h\}\\ \widehat{\alpha\beta}&=\frac{2p}{\pi D}(1-e^{-2\alpha})(1-e^{-4\alpha})\sin 2h\sin 2\beta\end{aligned}\right\}\quad\ldots\ldots\ldots\ldots(15a)$$

In the case where $2h$ is very small, we may put approximately

$$\sin 2h=2h$$
$$\cos 2h=1$$
$$\mathrm{tg}^{-1}[\sin 2h/(e^{2\alpha}+\cos 2h)]=2h/(1+e^{2\alpha})$$

Then the equation (15) may be written

$$\left.\begin{aligned}\widehat{\alpha\alpha}-\widehat{\beta\beta}-2i\widehat{\alpha\beta}&=\frac{8hp}{\pi D_1}(1-e^{-2\alpha})\Big[(1+e^{-4\alpha})\cos 2\beta\\ &\quad+2e^{-2\alpha}-i(1-e^{-4\alpha})\sin 2\beta\Big]\\ \widehat{\alpha\alpha}+\widehat{\beta\beta}&=\frac{2p}{\pi}\Big[\mathrm{tg}^{-1}\frac{2h\cos 2\beta+\sin 2\beta}{e^{2\alpha}+\cos 2\beta-2h\sin 2\beta}\\ &\quad+\mathrm{tg}^{-1}\frac{2h\cos 2\beta-\sin 2\beta}{e^{2\alpha}+\cos 2\beta+2h\sin 2\beta}-2h\Big]\end{aligned}\right\}\quad\ldots\ldots\ldots\ldots(16)$$

where $D_1=\{1+e^{-4\alpha}+2e^{-2\alpha}\cos 2\beta\}^2-\{4he^{-2\alpha}\sin 2\beta\}^2$

Hence on the horizontal diameter ($\beta=0$), we obtain

$$\widehat{\alpha\alpha}-\widehat{\beta\beta}-2i\widehat{\alpha\beta}=\frac{8hp}{\pi}\frac{1-e^{-2\alpha}}{(1+e^{-2\alpha})^2}$$
$$\widehat{\alpha\alpha}+\widehat{\beta\beta}=-\frac{4hp}{\pi}\frac{1-e^{-2\alpha}}{1+e^{-2\alpha}}$$

Solving these and putting

$$P=2habp$$
$$\xi=e^{-\alpha}=x/a$$

we have

$$\left.\begin{aligned}[\widehat{\alpha\alpha}]_{\beta=0}&=\frac{P}{\pi ab}\left\{\frac{1-\xi^2}{1+\xi^2}\right\}^2\\ [\widehat{\beta\beta}]_{\beta=0}&=-\frac{P}{\pi ab}\left\{\frac{4}{(1+\xi^2)^2}-1\right\}\\ [\widehat{\alpha\beta}]_{\beta=0}&=0\end{aligned}\right\}\quad\ldots\ldots\ldots\ldots(17)$$

On the vertical diameter $\left(\beta=-\frac{\pi}{2}\right)$ we have

$$\widehat{\alpha\alpha}-\widehat{\beta\beta}-2i\widehat{\alpha\beta}=-\frac{8hp}{\pi}\frac{1}{1-e^{-2\alpha}}$$
$$\widehat{\alpha\alpha}+\widehat{\beta\beta}=-\frac{4hp}{\pi}\frac{1+e^{-2\alpha}}{1-e^{-2\alpha}}$$

Solving these we obtain

$$\left.\begin{aligned}[\widehat{\alpha\alpha}]_{\beta=-\pi/2}&=-\frac{P}{\pi ab}\frac{3+\eta^2}{1-\eta^2}\\ [\widehat{\beta\beta}]_{\beta=-\pi/2}&=\frac{P}{\pi ab}\\ [\widehat{\alpha\beta}]_{\beta=-\pi/2}&=0\end{aligned}\right\}\quad\ldots\ldots\ldots\ldots(18)$$

where $\eta = e^{-\alpha} = y/a$

The equations (17) and (18) are in agreement with the results already given by previous authors[1] under the assumption of point loading. The results of these calculations are plotted in **Fig. 7.**

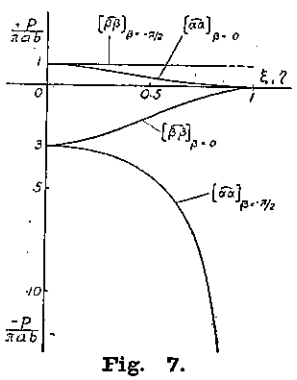

**Fig. 7.**

As a measure of the accuracy of the above reduction, the total pressure on the horizontal diameter is calculated by the pressure

$$2\int_0^a b[\widehat{\beta\beta}]_{\beta=0}\,dx = 2b\left(\frac{-P}{\pi ab}\right)\int_0^1 \left\{\frac{4}{(1+\xi^2)^2} - 1\right\} a\,d\xi$$
$$= -P$$

Thus the above expression for $\widehat{\beta\beta}$ in (17) is quite accurate on the horizontal diameter, while the stress $\widehat{\alpha\alpha}$ on the vertical diameter becomes infinite when $\eta = 1$.

## 11. Isoclinic and isochromatic lines.

In order to obtain the equation of isoclinic lines, the direction of the principal stress will be first considered. Let $\theta$ be the angle which the normal to one of the principal planes makes with the axis of $x$, and it is measured counter-clockwise from the positive direction of the said axis. Then we have the equation

$$\operatorname{tg} 2\theta = 2\tau/\{\sigma_x - \sigma_y\}\,.$$

In order to apply this equation to the present problem, we denote by $\varphi$ the angle between the normal to a principal plane and the radius vector passing through a given point. Then

$$\operatorname{tg} 2\varphi = 2\widehat{\alpha\beta}/\{\widehat{\alpha\alpha} - \widehat{\beta\beta}\}$$

$\varphi$ being measured counter-clockwise from the radius vector.

With the angle $\gamma$ which is equal to $-\beta$, the angle $\theta$ may be written

$$\theta = \gamma + \varphi$$
$$\varphi = \theta + \beta$$

Hence we get

$$\operatorname{tg} 2(\theta+\beta) = 2\widehat{\alpha\beta}/\{\widehat{\alpha\alpha} - \widehat{\beta\beta}\} \qquad \text{.....(19)}$$

Inserting (15a) into the right-hand member of (19), we have

$$\operatorname{tg} 2(\theta+\beta) = \frac{(1-e^{-4\alpha})\sin 2\beta}{(1+e^{-4\alpha})\cos 2\beta + 2e^{-2\alpha}\cos 2h}$$

This equation is satisfied by two values of $\theta$, differing by $\pi/2$, which may be called $\theta_1$ and $\theta_2$. From the above equation which is considered as a quadratic in $e^{-2\alpha}$, we obtain, in the case when $\cos 2h = 1$,

(1) Hertz, Michell, and Arakawa, *loc. cit.*

$$\left.\begin{aligned} e^{-2\alpha} &= -\sin\theta_1/\sin(\theta_1+2\beta) \\ e^{-2\alpha} &= -\cos\theta_2/\cos(\theta_2+2\beta) \end{aligned}\right\} \quad \ldots\ldots(20)$$

These two equations may be transformed into

$$y^2-x^2+2xy\cot\theta_1=a^2 \quad \ldots\ldots(21)$$

$$y^2-x^2-2xy\,\mathrm{tg}\,\theta_2=a^2 \quad \ldots\ldots(22)$$

respectively. These are the equations of the isoclinic line, $\theta_1$ and $\theta_2$ being the parameters.

If $x>0$ and $y>0$, we see from (21)

$$\cot\theta_1=\frac{a^2+x^2-y^2}{2xy}>0$$

while from (22)

$$\tan\theta_2=-\frac{a^2+x^2-y^2}{2xy}<0.$$

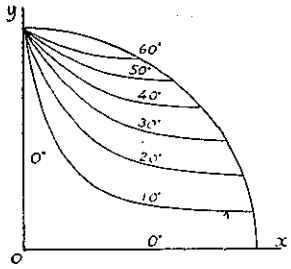


**Fig. 8.**

Thus a value of $\theta_1$ lying between zero and $\pi/2$ satisfies the first condition, and $\theta_2$ may be taken equal to $\theta_1+\pi/2$. Accordingly the equations (21) and (22) represent the same system of curves. We may take either of them to trace the isoclinic lines. **Fig. 8** shows the results of calculation for the first quadrant of the section, $\theta_1$ being taken as 0°, 10°, 20°, &c.

Next, the theory of elasticity shows that the principal stress difference $S$ at a point is connected with the stress-components by the relation

$$S=\left[(\widehat{\alpha\alpha}-\widehat{\beta\beta})^2+(2\widehat{\alpha\beta})^2\right]^{1/2}$$

Inserting the equations (15a) into the above, we have

$$S=\frac{4p\sin 2h}{\pi}\,\frac{1-e^{-2\alpha}}{D^{1/2}}$$

$$=\frac{2P\sin 2h}{\pi abh}\,\frac{1-e^{-2\alpha}}{D^{1/2}}.$$

As $Sb=Kn$, the order of extinction $n$ may be given by the following equation :—

$$n=\frac{4P}{\pi aK}\,\frac{\sin 2h}{2h}\,\frac{1-e^{-2\alpha}}{D^{1/2}} \quad \ldots\ldots(23)$$

where $K$ is the coefficient of photo-elastic extinction.

Neglecting the term containing $h^2$ in the expression for $D_1$ of the equations (16), we have approximately

$$D_1^{1/2}=1+e^{-4\alpha}+2e^{-2\alpha}\cos 2\beta.$$

Again putting $\sin 2h=2h$, we have from (23)

$$n=\frac{4P}{\pi aK}\,\frac{1-e^{-2\alpha}}{1+e^{-4\alpha}+2e^{-2\alpha}\cos 2\beta} \quad \ldots\ldots(24)$$

This is the equation of the isochromatic line for the present problem. Fig. 9 shows such lines obtained by calculation in the case where $4P/\pi aK=3$. In this figure, all lines touch with one another at the end of the vertical diameter. This is due to the approximation with which the equation (24) is derived.

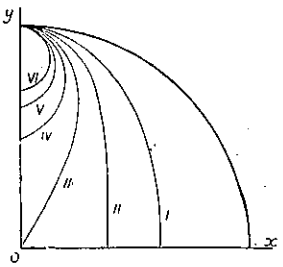

Fig. 9.

In order to obtain the exact expression for $n$ on the axis of $y$, we put $\beta=-\pi/2$ in (23). Then we get

$$n=\frac{4P}{\pi aK}\frac{\sin 2h}{2h}\frac{1-e^{-2a}}{1+e^{-4a}-2e^{-2a}\cos 2h}$$

or, with $\eta=e^{-a}=y/a$,

$$n=\frac{4P}{\pi aK}\frac{\sin 2h}{2h}\frac{1-\eta^2}{1+\eta^4-2\eta^2\cos 2h} \quad \cdots\cdots(25)$$

Differentiating $n$ of (25) with respect to $\eta$ and equating the result to zero, we have approximately

$$\eta_0=1-h \quad \cdots\cdots(26)$$

At this value of $\eta$, the equation (25) gives the maximum value of $n$, namely,

$$n=\frac{2P}{\pi aK}\frac{\cot h}{1-2h} \quad \cdots\cdots(27)$$

The highest order of extinction does not occur on the circumference of the circle.

## 12. Solution based on Hertz's theory of contact.

The elastic problem of stresses which arise when two cylinders, running parallel with each other, are pressed together was solved by M. T. Huber and S. Fuchs[1] in accordance with Hertz's general theory of contact. Now consider a special case where a cylinder $(E_1, \mu_1)$ is pressed on a plate $(E_2, \mu_2)$, where the bodies in the unstressed state are in contact with at the origin of $(x, y)$ and where the axis of $x$ is directed along the surface of the plate, the $z$-axis conforming in direction with the axis of the cylinder. Then the result given by Huber and Fuchs shows that the stress-distribution in the neibourhood of the origin can be represented by the equations

$$w^2=\frac{4p'a}{\pi}\left\{\frac{1-\mu_1^2}{E_1}+\frac{1-\mu_2^2}{E_2}\right\}$$

$$\sigma_x=\frac{2p'}{\pi}\frac{y}{w^2}\left\{\sqrt{\frac{v+w^2}{v}}\left(2-\frac{w^2y^2}{v^2+w^2y^2}\right)-2\right\}$$

(1) *loc. cit.*

$$\left.\begin{aligned}\sigma_y &= \frac{2p'}{\pi}\frac{y^3}{v^2+w^2y^2}\sqrt{\frac{v+w^2}{v}}\\ \sigma_z &= \frac{4p'\mu}{\pi}\frac{y}{w^2}\left\{\sqrt{\frac{v+w^2}{v}}-1\right\}\\ \tau &= \frac{2p'}{\pi}\frac{xy^2}{v^2+w^2y^2}\sqrt{\frac{v}{v+w^2}}\end{aligned}\right\} \quad \cdots\cdots(28)$$

where

$2v$ : $(x^2+y^2-w^2)+\sqrt{[(x^2+y^2-w^2)^2+4w^2y^2]}$

$2w$ : width of the contact area,

$a$ : radius of the cylinder,

$p'$ : applied load per unit length of the cylinder,

$E_1, E_2$ : YOUNG's moduli,

$\mu_1, \mu_2$ : POISSON's ratios.

On the axis of $y$, we have, by putting $x=0$ in (28),

$$\left.\begin{aligned}\sigma_x &= \frac{2p'}{\pi w^2}\left\{2(\sqrt{y^2+w^2}-y)-\frac{w^2}{\sqrt{y^2+w^2}}\right\}\\ \sigma_y &= \frac{2p'}{\pi w^2}\frac{w^2}{\sqrt{y^2+w^2}}\\ \sigma_z &= \frac{2p'}{\pi w^2}\left\{2\mu(\sqrt{y^2+w^2}-y)\right\}\\ \tau &= 0\end{aligned}\right\} \quad \cdots\cdots(29)$$

These normal stresses are the principal ones. Hence on the axis of $y$ the diffences of two principal stresses are as follows :—

$$\left.\begin{aligned}\sigma_y-\sigma_x &= \frac{4p'}{\pi w}\left[\frac{w}{\sqrt{y^2+w^2}}-\frac{\sqrt{y^2+w^2}-y}{w}\right]\\ \sigma_z-\sigma_x &= \frac{4p'}{\pi w}\left[\frac{1}{2}\frac{w}{\sqrt{y^2+w^2}}-(1-\mu)\frac{\sqrt{y^2+w^2}-y}{w}\right]\\ \sigma_y-\sigma_z &= \frac{4p'}{\pi w}\left[\frac{1}{2}\frac{w}{\sqrt{y^2+w^2}}-\mu\frac{\sqrt{y^2+w^2}-y}{w}\right]\end{aligned}\right\} \quad \cdots\cdots(30)$$

In order to determine the order of magnitude of the above three expressions, the coefficients of $4p'/\pi w$ are calculated for several values of $y$ as shown in the next table. In preparing the table, a phenolite cylinder is considered as an example and the value of $\mu$ is taken at 0.36 as shown in Chapter 2.

| Value of | Coefficients of $\frac{4p'}{\pi w}$ in the expressions of | | |
|---|---|---|---|
| $y$ | $\sigma_y-\sigma_x$ | $\sigma_z-\sigma_x$ | $\sigma_y-\sigma_z$ |
| 0 | 0 | −0.14 | 0.14 |
| 0.5 $w$ | 0.27 | 0.05 | 0.23 |
| 1 $w$ | 0.30 | 0.09 | 0.20 |
| 2 $w$ | 0.21 | 0.07 | 0.13 |
| 3 $w$ | 0.16 | 0.06 | 0.10 |

| | | | |
|---|---|---|---|
| 4 $w$ | 0.12 | 0.04 | 0.08 |
| 5 $w$ | 0.10 | 0.03 | 0.06 |
| 10 $w$ | 0.05 | 0.02 | 0.03 |

It may be found from this table that the value of $(\sigma_y-\sigma_x)$ is greater than those of the other two expressions.

Differentiating $(\sigma_y-\sigma_x)$ with respect to $y$ and equating the result to zero, we have $y_1$ as a value of $y$

$$y_1=0.786w$$

At this point, $(\sigma_y-\sigma_x)$ becomes a maximum, its value being

$$(\sigma_y-\sigma_x)=0.300\frac{4p'}{\pi w}$$

As **Fig. 9** shows, the highest order of extinction in the whole section occurs on the axis of compression. It may be here said that the maximum given by the above equation is the greatest value of the principal stress difference in the section.

Putting $w=h_1a$, and denoting the distance between the point of the maximum and the centre of the circle by $\eta_1 a$, we get

$$\eta_1=1-\frac{y_1}{a}=1-0.786h_1 \quad \cdots\cdots(31)$$

$h_1$ being the angle at the centre made by the arc $w$. As we may write $(\sigma_y-\sigma_x)\times b=Kn$ on the axis of $y$, the highest order of extinction $n$ is given by the equation

$$n=0.300\frac{4p'}{\pi w}\frac{b}{K}$$

$$=\frac{2p'b}{\pi aK}\frac{0.6}{h_1} \quad \cdots\cdots(32)$$

The equation (31) corresponds to (26) given in the previous article, although they are not in thorough agreement with each other, owing to the fact that the distribution of the applied load differs in the two cases. Nevertheless, it is ascertained from the two equations that the greatest shearing stress in the section occurs at a point on the axis of compression lying a little inside the circumference.

## 13. Experiment.

The photo-elastic observation was carried out by means of the apparatus as shown in **Figs, 10** and **11**. In this apparatus a mercury vapour lamp is used as a

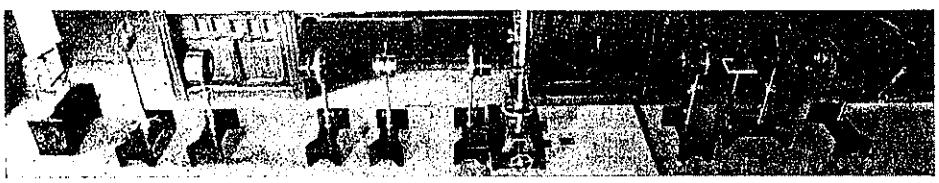

**Fig. 10.**

light source. The polarizer and analyzer consist of GLAN-THOMPSON prisms supplied by *Carl Zeiss & Co.* The beam of light from the source reaches the specimen after passing through a condenser, a lens, the polarizer and a lens in succession. The specimen is then projected by a lens on a dry plate in a camera through a shutter. The analyzer and a Wratten light filter No. 77*A* are placed in front of the camera. The focal length of each of the three lenses mentioned above is 30 cm, the relative aperture being *F*/4.5. The quarter-wave plates installed in the polarizer and the analyzer are easily removable from them.

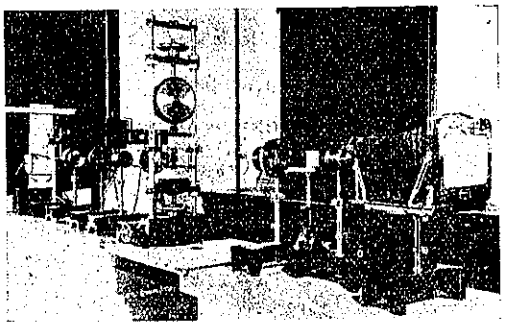

Fig. 11.

A circular disc of phenolite, 35 mm in diameter and 6 mm in thickness, was compressed by means of a device as shown in **Fig. 12**. The disc was annealed before the test to remove the initial stress. The isochromatic lines were photographed at the instant 1 minute after loading (**Fig. 13**), the load applied being 43.7 kg. At the instant 15 minutes after loading, **Fig. 14** was taken under the same load.

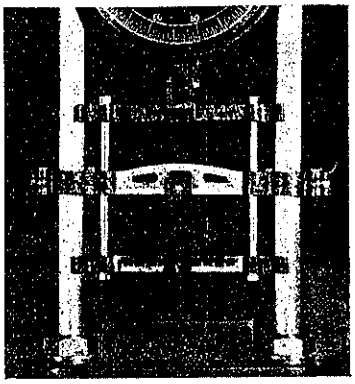

Fig. 12.

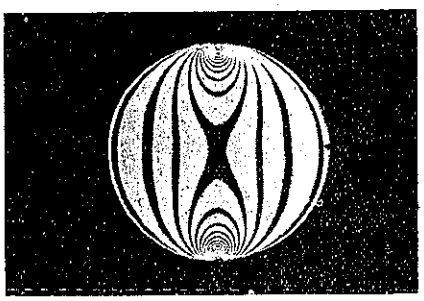

Fig. 13.

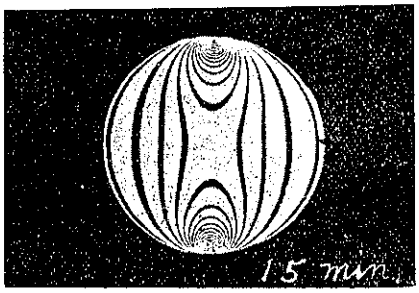


Fig. 14.

If the coefficient of photo-elastic extinction $K_1$ is taken at 10.6 kg/cm as shown in Chapter 1, we have in this case

$$4P/\pi aK=3$$

which agrees with the relation assumed in preparing the theoretical isochromatic lines shown in **Fig. 9.** Thus **Fig. 13** should be compared with **Fig. 9.**

The comparison of **Fig. 13** with **Fig. 14** shows that the isochromatic lines taken

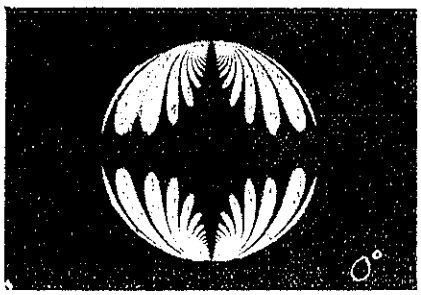


Fig. 15.

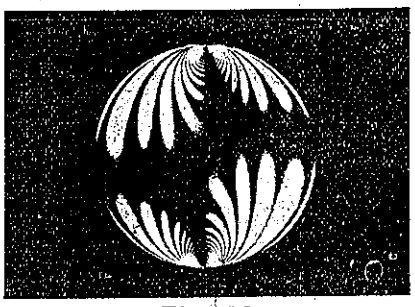


Fig. 16.

at the instant 15 minutes after loading differ from those obtained 1 minute after loading, particularly in the central part of the figure.

On removing the quarter-wave plates from the apparatus, the isoclinic lines were photographed as represented by the dark broad bands, for example, of **Figs. 15, 16** and **17**. With these bands the theoretical lines, **Fig. 8**, are to be compared.

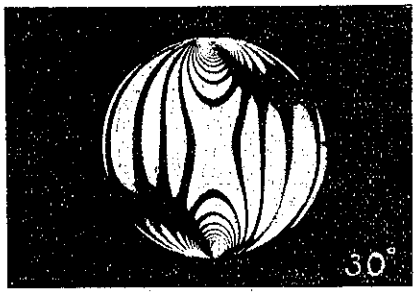


Fig. 17.

For photographing the isochromatic and isoclinic lines, *the Ilford Screened Chromatic Plates* were used, the time of exposure being a tenth of a second.

The isochromatic line of the highest order surrounds a point which is a little distant from the periphery (**Fig. 13**), the distance between this point and the centre of the circle being measured to be 0.96 times the radius. In order to compare this observed value with the calculated one given by (31), the elastic constants are taken as follows:—

$$E_1 = 4.3 \times 10^4\ kg/cm^2, \quad \mu_1 = 0.36 \quad \text{for phenolite,}$$

$$E_2 = 2 \times 10^6\ kg/cm^2, \quad \mu_2 = 0.3 \quad \text{for steel.}$$

With $P/b = p' = 72.8$ kg/cm, we have from the first equation of (28)

$$w = 0.332\, a,$$

and from (31)

$$\eta_1 = 0.974.$$

The point of the greatest shearing stress can not be so acculately determined trom the photograph that the observation and the calculation may exactly coincide. Moreover, it is hardly necessary to add that the cylinder considered in HERTZ's fheory is a long one, while the disc here tested is comparatively thin and should be considered as a problem of generalized plane stress.

## Chapter 4. Rectangular Plate Compressed on Two Opposite Sides.

### 14. Solution of the problem.

In the case of a rectangular plate, it is found difficult to make use of the method applied in the preceding chapter. Hence the present problem is solved by means of AIRY's stress-function $F$, which satisfies the differential equation

$$\frac{\partial^4 F}{\partial x^4}+2\frac{\partial^4 F}{\partial x^2 \partial y^2}+\frac{\partial^4 F}{\partial y^4}=0.$$

The stress-components may be expressed by the equations

$$\sigma_x=\frac{\partial^2 F}{\partial y^2}, \quad \sigma_y=\frac{\partial^2 F}{\partial x^2}, \quad \tau=-\frac{\partial^2 F}{\partial x \partial y} \qquad \ldots\ldots(1)$$

In a rectangular plate subjected to symmetrical loads as shown in **Fig. 18**, we have to satisfy the conditions that the normal and shearing stresses on the boundary surface are zero except at the region where the load acts. Thus there are eight conditions

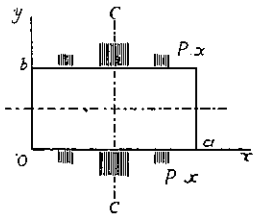

Fig. 18.

(i) $\quad [\sigma_x]_{x=0}=[\sigma_x]_{x=a}=0$

(ii) $\quad [\sigma_y]_{y=0}=[\sigma_y]_{y=b}=-P(x)$

(iii) $\quad [\tau]_{x=0}=[\tau]_{x=a}=0$

(iv) $\quad [\tau]_{y=0}=[\tau]_{y=b}=0$

The load $P(x)$ on the side $y=b$ is assumed to be quite the same as that on the side $y=0$, and both loads are symmetrical about the centre line $C$-$C$. $P(x)$ being given in the interval $(0, a)$, it may be represented in the form

$$P(x)=\frac{4P_1}{\pi}\sum_{n=1}^{\infty}A_n' \sin\frac{n\pi x}{a} \qquad \ldots\ldots(2)$$

where

$$\frac{4P_1}{\pi}A_n'=\frac{2}{a}\int_0^a P(x)\sin\frac{n\pi x}{a}dx$$

and $P_1$ is the value of $P(x)$ at a chosen point.

As $P(x)$ is assumed to be symmetrical about $x=a/2$, the terms containing sines of even multiples of $\pi x/a$ disappear, and we may take odd values of $n$ in (2).

Now we take a stress-function $F$ as follows:—

$$F=F_1+F_2+F_3 \qquad \ldots\ldots(3)$$

where

$$F_1=\frac{4P_1}{\pi}\sum_{n=1}^{\infty}A_n\frac{a^2}{n^2\pi^2}\operatorname{Sech}\frac{n\pi b}{2a}\operatorname{Cosh}\frac{n\pi}{a}\left(y-\frac{b}{2}\right)\sin\frac{n\pi x}{a}$$

$$F_2=\frac{4P_1}{\pi}\sum_{n=1}^{\infty}B_n\frac{a^2}{n^2\pi^2}\left(\frac{n\pi b}{a}+\operatorname{Sinh}\frac{n\pi b}{a}\right)^{-1}\left\{\frac{n\pi y}{a}\operatorname{Sinh}\frac{n\pi(y-b)}{a}\right.$$
$$\left.+\frac{n\pi(y-b)}{a}\operatorname{Sinh}\frac{n\pi y}{a}\right\}\sin\frac{n\pi x}{a}$$

$$F_3=\frac{4P_1}{\pi}\sum_{n=1}^{\infty}C_n\frac{b^2}{n^2\pi^2}\left(\frac{n\pi a}{b}+\operatorname{Sinh}\frac{n\pi a}{b}\right)^{-1}\left\{\frac{n\pi x}{b}\operatorname{Sinh}\frac{n\pi(x-a)}{b}\right.$$
$$\left.+\frac{n\pi(x-a)}{b}\operatorname{Sinh}\frac{n\pi x}{b}\right\}\sin\frac{n\pi y}{b}$$

In these expressions $n$ is assumed to be odd to conform to the boundary conditions.

As

$$\left.\begin{aligned}
\frac{\partial^2F_1}{\partial y^2}&=\frac{4P_1}{\pi}\sum_{n=1}^{\infty}A_n\operatorname{Sech}\frac{n\pi b}{2a}\operatorname{Cosh}\frac{n\pi}{a}\left(y-\frac{b}{2}\right)\sin\frac{n\pi x}{a}\\
\frac{\partial^2F_2}{\partial y^2}&=\frac{4P_1}{\pi}\sum_{n=1}^{\infty}B_n\left(\frac{n\pi b}{a}+\operatorname{Sinh}\frac{n\pi b}{a}\right)^{-1}\left\{2\operatorname{Cosh}\frac{n\pi(y-b)}{a}+2\operatorname{Cosh}\frac{n\pi y}{a}\right.\\
&\quad\left.+\frac{n\pi y}{a}\operatorname{Sinh}\frac{n\pi(y-b)}{a}+\frac{n\pi(y-b)}{a}\operatorname{Sinh}\frac{n\pi y}{a}\right\}\sin\frac{n\pi x}{a}\\
\frac{\partial^2F_3}{\partial y^2}&=-\frac{4P_1}{\pi}\sum_{n=1}^{\infty}C_n\left(\frac{n\pi a}{b}+\operatorname{Sinh}\frac{n\pi a}{b}\right)^{-1}\left\{\frac{n\pi x}{b}\operatorname{Sinh}\frac{n\pi(x-a)}{b}\right.\\
&\quad\left.+\frac{n\pi(x-a)}{b}\operatorname{Sinh}\frac{n\pi x}{b}\right\}\sin\frac{n\pi y}{b}
\end{aligned}\right\}\quad\cdots\cdots(4)$$

$\sigma_x$ vanishes for $x=0$ and $x=a$ respectively. Hence the boundary conditions (i) are satisfied.

Next referring to the conditions (ii), we have

$$\left.\begin{aligned}
\frac{\partial^2F_1}{\partial x^2}&=-\frac{4P_1}{\pi}\sum_{n=1}^{\infty}A_n\operatorname{Sech}\frac{n\pi b}{2a}\operatorname{Cosh}\frac{n\pi}{a}\left(y-\frac{b}{2}\right)\sin\frac{n\pi x}{a}\\
\frac{\partial^2F_2}{\partial x^2}&=-\frac{4P_1}{\pi}\sum_{n=1}^{\infty}B_n\left(\frac{n\pi b}{a}+\operatorname{Sinh}\frac{n\pi b}{a}\right)^{-1}\left\{\frac{n\pi y}{a}\operatorname{Sinh}\frac{n\pi(y-b)}{a}\right.\\
&\quad\left.+\frac{n\pi(y-b)}{a}\operatorname{Sinh}\frac{n\pi y}{a}\right\}\sin\frac{n\pi x}{a}\\
\frac{\partial^2F_3}{\partial x^2}&=\frac{4P_1}{\pi}\sum_{n=1}^{\infty}C_n\left(\frac{n\pi a}{b}+\operatorname{Sinh}\frac{n\pi a}{b}\right)^{-1}\left\{2\operatorname{Cosh}\frac{n\pi(x-a)}{b}\right.\\
&\quad+2\operatorname{Cosh}\frac{n\pi x}{b}+\frac{n\pi x}{b}\operatorname{Sinh}\frac{n\pi(x-a)}{b}\\
&\quad\left.+\frac{n\pi(x-a)}{b}\operatorname{Sinh}\frac{n\pi x}{b}\right\}\sin\frac{n\pi y}{b}
\end{aligned}\right\}\quad\cdots\cdots(5)$$

The second and third expressions of (5) vanish for $y=b$ as well as $y=0$. Thus

$$\left[\frac{\partial^2 F}{\partial x^2}\right]_{y=0}=\left[\frac{\partial^2 F}{\partial x^2}\right]_{y=b}=-\frac{4P_1}{\pi}\sum_{n=1}^{\infty}A_n\sin\frac{n\pi x}{a} \quad \ldots\ldots(6)$$

To satisfy the conditions (ii), we have to put from (2) and (6)

$$A_n=A_n' \quad \ldots\ldots(7)$$

In regard to the shearing stress $\tau$, we have

$$\left.\begin{aligned}
\frac{\partial^2 F_1}{\partial x\partial y}&=\frac{4P_1}{\pi}\sum_{n=1}^{\infty}A_n\,\mathrm{Sech}\frac{n\pi b}{2a}\,\mathrm{Sinh}\frac{n\pi}{a}\left(y-\frac{b}{2}\right)\cos\frac{n\pi x}{a}\\
\frac{\partial^2 F_2}{\partial x\partial y}&=\frac{4P_1}{\pi}\sum_{n=1}^{\infty}B_n\left(\frac{n\pi b}{a}+\mathrm{Sinh}\frac{n\pi b}{a}\right)^{-1}\left\{\mathrm{Sinh}\frac{n\pi(y-b)}{a}+\mathrm{Sinh}\frac{n\pi y}{a}\right.\\
&\quad\left.+\frac{n\pi y}{a}\,\mathrm{Cosh}\frac{n\pi(y-b)}{a}+\frac{n\pi(y-b)}{a}\,\mathrm{Cosh}\frac{n\pi y}{a}\right\}\cos\frac{n\pi x}{a}\\
\frac{\partial^2 F_3}{\partial x\partial y}&=\frac{4P_1}{\pi}\sum_{n=1}^{\infty}C_n\left(\frac{n\pi a}{b}+\mathrm{Sinh}\frac{n\pi a}{b}\right)^{-1}\left\{\mathrm{Sinh}\frac{n\pi(x-a)}{b}+\mathrm{Sin}\frac{n\pi x}{b}\right.\\
&\quad\left.+\frac{n\pi x}{b}\,\mathrm{Cosh}\frac{n\pi(x-a)}{b}+\frac{n\pi(x-a)}{b}\,\mathrm{Cosh}\frac{n\pi x}{b}\right\}\cos\frac{n\pi x}{b}
\end{aligned}\right\}\quad\ldots\ldots(8)$$

Putting $x=0$ in (8), we have

$$\left.\begin{aligned}
\left[\frac{\partial^2 F_1}{\partial x\partial y}\right]_{x=0}&=\frac{4P_1}{\pi}\sum_{n=1}^{\infty}A_n\,\mathrm{Sech}\frac{n\pi b}{2a}\,\mathrm{Sinh}\frac{n\pi}{a}\left(y-\frac{b}{2}\right)\\
\left[\frac{\partial^2 F_2}{\partial x\partial y}\right]_{x=0}&=\frac{4P_1}{\pi}\sum_{n=1}^{\infty}B_n\left(\frac{n\pi b}{a}+\mathrm{Sinh}\frac{n\pi b}{a}\right)^{-1}\left\{\mathrm{Sinh}\frac{n\pi(y-b)}{a}\right.\\
&\quad\left.+\mathrm{Sinh}\frac{n\pi y}{a}+\frac{n\pi y}{a}\,\mathrm{Cosh}\frac{n\pi(y-b)}{a}+\frac{n\pi(y-b)}{a}\,\mathrm{Cosh}\frac{n\pi y}{a}\right\}\\
\left[\frac{\partial^2 F_3}{\partial x\partial y}\right]_{x=0}&=-\frac{4P_1}{\pi}\sum_{n=1}^{\infty}C_n\cos\frac{n\pi y}{b}
\end{aligned}\right\}\quad\ldots\ldots(9)$$

Expanding $\mathrm{Sinh}\frac{n\pi}{a}\left(y-\frac{b}{2}\right)$ in the first expression in FOURIER's cosine series, we have

$$\begin{aligned}
&\left[\frac{\partial^2 F_1}{\partial x\partial y}\right]_{x=0}\\
&=\frac{4P_1}{\pi}\sum_{r=1}^{\infty}A_r\,\mathrm{Sech}\frac{r\pi b}{2a}\sum_{n=1}^{\infty}\frac{2}{\pi}\frac{rab}{n^2a^2+r^2b^2}(\cos n\pi-1)\,\mathrm{Cosh}\frac{r\pi b}{2a}\cos\frac{n\pi y}{b}\\
&=-\frac{4P_1}{\pi}\sum_{r=1}^{\infty}\sum_{n=1}^{\infty}A_r\frac{4}{\pi}\frac{rab}{n^2a^2+r^2b^2}\cos\frac{n\pi y}{b}
\end{aligned}$$

$n$ and $r$ being odd numbers.

By a similar process, the second expression of (9) can be transformed into the form

$$\begin{aligned}
&\left[\frac{\partial^2 F_2}{\partial x\partial y}\right]_{x=0}\\
&=\frac{4P_1}{\pi}\sum_{r=1}^{\infty}\frac{B_r}{\frac{r\pi b}{a}+\mathrm{Sinh}\frac{r\pi b}{a}}\sum_{n=1}^{\infty}\frac{-8}{\pi}\frac{n^2ra^3b}{(n^2a^2+r^2b^2)^2}\left(1+\mathrm{Cosh}\frac{r\pi b}{a}\right)\cos\frac{n\pi y}{b}
\end{aligned}$$

$$= -\frac{4P_1}{\pi}\sum_{r=1}^{\infty}\sum_{n=1}^{\infty} B_r \frac{8}{\pi}\frac{n^2ra^3b}{(n^2a^2+r^2b^2)^2}\frac{1+\mathrm{Cosh}\frac{r\pi b}{a}}{\frac{r\pi b}{a}+\mathrm{Sinh}\frac{r\pi b}{a}}\cos\frac{n\pi y}{b}$$

where $n$ and $r$ are odd.

Now put, for simplicity,

$$\left.\begin{aligned} Y_{nr} &= \frac{4}{\pi}\frac{rab}{n^2a^2+r^2b^2} \\ Z_{nr}\left(\frac{b}{a}\right) &= \frac{8}{\pi}\frac{n^2ra^3b}{(n^2a^2+r^2b^2)^2}\left(1+\mathrm{Cosh}\frac{r\pi b}{a}\right)\left(\frac{r\pi b}{a}+\mathrm{Sinh}\frac{r\pi b}{a}\right)^{-1} \end{aligned}\right\} \quad \cdots\cdots\cdots(10)$$

Adding the three equations of (9), we have with (10)

$$\left[\frac{\partial^2 F}{\partial x\partial y}\right]_{x=0} = -\frac{4P_1}{\pi}\sum_{n=1}^{\infty}\left[\sum_{r=1}^{\infty}\left\{A_rY_{nr}+B_rZ_{nr}\left(\frac{b}{a}\right)\right\}+C_n\right]\cos\frac{n\pi y}{b}$$

If the terms enclosed with square brackets in the above equation are equal to zero, the first condition of (iii) is satisfied. So we put

$$C_n+\sum_{r=1}^{\infty}\left\{A_rY_{nr}+B_rZ_{nr}\left(\frac{b}{a}\right)\right\}=0 \quad \cdots\cdots\cdots\cdots\cdots\cdots\cdots\cdots\cdots\cdots\cdots\cdots(11)$$

where $B_r$ and $C_n$ are still unknow.

As to the second condition of (iii), it is easily seen that

$$\left[\frac{\partial^2 F}{\partial x\partial y}\right]_{x=a} = -\left[\frac{\partial^2 F}{\partial x\partial y}\right]_{x=0}$$

Thus the condition is also expressed by (11).

Next, putting $y=0$ in (8), we get

$$\left[\frac{\partial^2 F_1}{\partial x\partial y}\right]_{y=0} = -\frac{4P_1}{\pi}\sum_{n=1}^{\infty} An\,\mathrm{Tanh}\frac{n\pi b}{2a}\cos\frac{n\pi x}{a}$$

$$\left[\frac{\partial^2 F_2}{\partial x\partial y}\right]_{y=0} = -\frac{4P_1}{\pi}\sum_{n=1}^{\infty} B_1\cos\frac{n\pi x}{a}$$

$$\left[\frac{\partial^2 F_3}{\partial x\partial y}\right]_{y=0} = \frac{4P_1}{\pi}\sum_{n=1}^{\infty} C_n\left(\frac{n\pi a}{b}+\mathrm{Sinh}\frac{n\pi a}{b}\right)^{-1}\left\{\mathrm{Sinh}\frac{n\pi(x-a)}{b}+\mathrm{Sinh}\frac{n\pi x}{b}\right.$$

$$\left.+\frac{n\pi x}{b}\mathrm{Cosh}\frac{n\pi(x-a)}{b}+\frac{n\pi(x-a)}{b}\mathrm{Cosh}\frac{n\pi x}{b}\right\}$$

The last expression can be transformed into the form

$$\left[\frac{\partial^2 F_3}{\partial x\partial y}\right]_{y=0} = \frac{4P_1}{\pi}\sum_{r=1}^{\infty}\frac{C_r}{\frac{r\pi a}{b}+\mathrm{Sinh}\frac{r\pi a}{b}}\sum_{n=1}^{\infty}\frac{-8}{\pi}\frac{n^2rab^3}{(n^2b^2+r^2a^2)^2}\left(1+\mathrm{Cosh}\frac{r\pi a}{b}\right)\cos\frac{n\pi x}{a}$$

$$= -\frac{4P_1}{\pi}\sum_{r=1}^{\infty}\sum_{n=1}^{\infty} C_rZ_{nr}\left(\frac{a}{b}\right)\cos\frac{n\pi x}{a}$$

where

$$Z_{nr}\left(\frac{a}{b}\right) = \frac{8}{\pi}\frac{n^2rab^3}{(n^2b^2+r^2a^2)^2}\left(1+\mathrm{Cosh}\frac{r\pi a}{b}\right)\left(\frac{r\pi a}{b}+\mathrm{Sinh}\frac{r\pi a}{b}\right)^{-1} \quad \cdots\cdots\cdots\cdots(12)$$

Hence we have

$$\left[\frac{\partial^2 F}{\partial x \partial y}\right]_{y=0} = -\frac{4P_1}{\pi}\sum_{n=1}^{\infty}\left[A_n \operatorname{Tanh}\frac{n\pi b}{2a} + B_n + \sum_{r=1}^{\infty} C_r Z_{nr}\left(\frac{a}{b}\right)\right]\cos\frac{n\pi x}{a}$$

In order that the first condition of (iv) may be satisfied, we have to put

$$B_n + \sum_{r=1}^{\infty} C_r Z_{nr}\left(\frac{a}{b}\right) + A_n \operatorname{Tanh}\frac{n\pi b}{2a} = 0 \quad \cdots\cdots(13)$$

The other condition of (iv) will be also satisfied by (13) as

$$\left[\frac{\partial^2 F}{\partial x \partial y}\right]_{y=b} = -\left[\frac{\partial^2 F}{\partial x \partial y}\right]_{y=0}$$

$A_n$ being given by (7), $B_n$ and $C_n$ are found by solving the two systems of equations (11) and (13) simultaneously. As each of the latter equations contains two series of unknowns in it, the numerical calculation is extremely tedious. To obtain a system of equations which involves a series of unknowns, we write by (13)

$$B_r = -\sum_{s=1}^{\infty} C_r Z_{rs}\left(\frac{a}{b}\right) - A_r \operatorname{Tanh}\frac{r\pi b}{2a}$$

Inserting this expression into (11), we get

$$C_n - \sum_{r=1}^{\infty}\sum_{s=1}^{\infty} C_s Z_{nr}\left(\frac{b}{a}\right) Z_{rs}\left(\frac{a}{b}\right) = \sum_{r=1}^{\infty} A_r\left\{Z_{nr}\left(\frac{b}{a}\right)\operatorname{Tanh}\frac{r\pi b}{2a} - Y_{nr}\right\} \quad \cdots\cdots(14)$$

As the right-hand member of (14) is known by finding $A_n$, the equations, which are simultaneous ones of the first degree involving infinite number of unknowns, can be solved approximately by the method of iteration. On finding $C_n$, the values of $B_n$ are obtained from (13).

When the coefficients $A_n$, $B_n$ and $C_n$ are known, the stress-components at a point are determined from (1).

## 15. Numerical example.

As an example of the above solution, a square plate whose side is $a$ is supposed to be compressed by a pair of uniform loads distributed over the length of $a/5$ with the intensity $p$ as shown in **Fig. 19.** Thus we have

$$P(x) = p \quad \text{for} \quad 0.4\,a \leqq x \leqq 0.6\,a$$
$$P(x) = 0 \quad \text{for} \quad x < 0.4\,a \quad \text{and} \quad x > 0.6\,a$$

The sine series representing $P(x)$ is then

$$P(x) = \frac{4p}{\pi}\sum_{n=1}^{\infty}\frac{1}{n}\sin\frac{n\pi}{2}\sin\frac{n\pi}{10}\sin\frac{n\pi x}{a}$$

Comparing this with (2) and (7), we have

$$P_1 = p$$
$$A_n = A'_n = \frac{1}{n}(-1)^{\frac{n-1}{2}}\sin\frac{n\pi}{10}$$

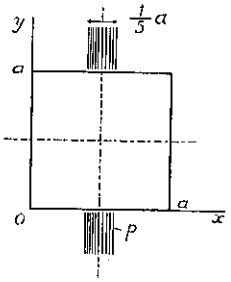


Fig. 19.

| $n$ | $A_n$ | $-B_n$ | $-C_n$ |
|---|---|---|---|
| 1 | 0.3091 | 0.2652 | 0.0396 |
| 3 | −0.2697 | −0.2803 | 0.0112 |
| 5 | 0.2000 | 0.1923 | 0.0139 |
| 7 | −0.1156 | −0.1211 | 0.0099 |
| 9 | 0.0343 | 0.0292 | 0.0071 |
| 11 | 0.0281 | 0.0238 | 0.0056 |
| 13 | −0.0622 | −0.0660 | 0.0045 |
| 15 | 0.0667 | 0.0639 | 0.0038 |
| 17 | −0.0476 | −0.0504 | 0.0032 |
| 19 | 0.0163 | 0.0137 | 0.0028 |
| 21 | 0.0147 | 0.0123 | 0.0025 |
| 23 | −0.0352 | −0.0373 | 0.0023 |
| 25 | 0.0400 | 0.0381 | 0.0020 |

Table 1.

$n$ being odd. The values of $A_n$ are calculated as shown in **Table 1.** As $a=b$, we have from (10) and (12)

$$Y_{nr}=\frac{4}{\pi}\frac{r}{n^2+r^2}$$

$$Z_{nr}\left(\frac{b}{a}\right)=Z_{nr}\left(\frac{a}{b}\right)=\frac{8}{\pi}\frac{n^2 r}{(n^2+r^2)^2}(1+\operatorname{Cosh} r\pi)(r\pi+\operatorname{Sinh} r\pi)^{-1}$$

If we put

$$\left.\begin{aligned}\alpha_{ns}&=\sum_{r=1}^{\infty}Z_{nr}Z_{rs}\\ \beta_n&=\sum_{r=1}^{\infty}A_r\left\{Z_{nr}\operatorname{Tanh}\frac{r\pi}{2}-Y_{nr}\right\}\end{aligned}\right\}\quad\ldots\ldots\ldots\ldots\ldots\ldots\ldots\ldots\ldots\ldots(15)$$

we may write (14) in the form

$$C_n-\sum_{s=1}^{\infty}\alpha_{ns}C_s=\beta_n$$

or

$$\left.\begin{aligned}&C_1-\{\alpha_{11}C_1+\alpha_{13}C_3+\alpha_{15}C_5+\alpha_{17}C_7+\ldots.\}=\beta_1\\ &C_3-\{\alpha_{31}C_1+\alpha_{33}C_3+\alpha_{35}C_5+\alpha_{37}C_7+\ldots.\}=\beta_3\\ &C_5-\{\alpha_{51}C_1+\alpha_{53}C_3+\alpha_{55}C_5+\alpha_{57}C_7+\ldots.\}=\beta_5\\ &C_7-\{\alpha_{71}C_1+\alpha_{73}C_3+\alpha_{75}C_5+\alpha_{77}C_7+\ldots.\}=\beta_7\\ &\ldots\ldots\ldots\ldots\ldots\\ &\ldots\ldots\ldots\ldots\ldots\end{aligned}\right\}\quad\ldots\ldots\ldots\ldots\ldots\ldots\ldots\ldots\ldots\ldots(16)$$

To solve the simultaneous equations (16), we first neglect $C_3$, $C_5$, .... in the first one, and find $C_1'$, the first approximate value of $C_1$, from the equation

$$(1-\alpha_{11})C_1'=\beta_1$$

Inserting $C_1'$ into the second equation and neglecting $C_5$, $C_7$, ...., we find $C_3'$, the first approximate value of $C_3$, from the equation

$$(1-\alpha_{33})C_3'=\beta_3+\alpha_{31}C_1'$$

Inserting $C_1'$ and $C_3'$ into the third equation and neglecting $C_7$, $C_9$, ...., we

find $C_5'$, the first approximate value of $C_5$, from the equation

$$(1-\alpha_{55})C_5' = \beta_5 + \alpha_{51}C_1' + \alpha_{53}C_3'$$

By a similar procedure, we find $C_7'$, $C_9'$, .... as the first approximate values of $C_7$, $C_9$, ...., respectively.

In the second step, we insert $C_3'$, $C_5'$, .... into the first equation of (16) and find $C_1''$, the second approximate value of $C_1$, from the equation

$$(1-\alpha_{11})C_1'' = \beta_1 + \alpha_{13}C_3' + \alpha_{15}C_5' + \alpha_{17}C_7' + \cdots\cdots\cdots\cdots$$

Inserting $C_1''$, $C_5'$, $C_7'$, .... into the second equation, we find $C_3''$, the second approximate value of $C_3$, from the equation

$$(1-\alpha_{33})C_3'' = \beta_3 + \alpha_{31}C_1'' + \alpha_{35}C_5' + \alpha_{37}C_7' + \cdots\cdots\cdots\cdots$$

By a similar process, we find $C_5''$, $C_7''$, .... as the second approximate values of $C_5$, $C_7$, ...., respectively.

The third, the fourth, .... approximate values of $C_n$ are found successively. Such trials are repeated until the precision of the values of $C_n$ is secured in the decimal place specified.

In the actual calculation, $n$ and $s$ are taken up to 25, and $r$ is up to 79. Although higher values of $r$ than this are needed to secure the accuracy of $\alpha_{ns}$ and $\beta_n$, the calculation is too lengthy to do so. $\alpha_{ns}$ and $\beta_n$ calculated by (15) are given in **Table 2**, where the last figure of each value is not sufficiently accurate. On finding $C_n$, the values of $B_n$ are determined from (13), the results being given in **Table 1.** The last figures of $B_n$ and $C_n$ may not be sufficiently accurate.

| | $\alpha_{ns}$ | | | | | | | | | | | | | $-\beta_n$ |
|---|---|---|---|---|---|---|---|---|---|---|---|---|---|---|
| $s=$ | 1 | 3 | 5 | 7 | 9 | 11 | 13 | 15 | 17 | 19 | 21 | 23 | 25 | |
| | 0.0 | 0.0 | 0.0 | 0.0 | 0.0 | 0.0 | 0.0 | 0.0 | 0.0 | 0.0 | 0.0 | 0.0 | 0.0 | 0.0 |
| $n=1$ | 19729 | 5326 | 1940 | 0949 | 0540 | 0338 | 0229 | 0161 | 0118 | 0090 | 0070 | 0055 | 0045 | 3471 |
| 3 | 10773 | 8185 | 4641 | 2835 | 1850 | 1277 | 0921 | 0688 | 0529 | 0416 | 0334 | 0262 | 0225 | 0476 |
| 5 | 06568 | 7776 | 5313 | 3662 | 2606 | 1918 | 1453 | 1129 | 0894 | 0721 | 0594 | 0498 | 0415 | 0386 |
| 7 | 04493 | 6619 | 5115 | 3843 | 2920 | 2256 | 1784 | 1434 | 1166 | 0960 | 0821 | 0683 | 0583 | 0567 |
| 9 | 03267 | 5556 | 4669 | 3753 | 2994 | 2413 | 1963 | 1621 | 1350 | 1137 | 0969 | 0836 | 0719 | 0358 |
| 11 | 02506 | 4686 | 4201 | 3560 | 2950 | 2452 | 2048 | 1729 | 1468 | 1259 | 1085 | 0944 | 0827 | 0244 |
| 13 | 0199 | 399 | 378 | 331 | 284 | 239 | 207 | 177 | 152 | 129 | 115 | 101 | 088 | 0174 |
| 15 | 0162 | 344 | 339 | 307 | 270 | 234 | 202 | 176 | 154 | 136 | 123 | 106 | 095 | 0131 |
| 17 | 0134 | 299 | 302 | 281 | 253 | 224 | 199 | 178 | 155 | 139 | 124 | 110 | 099 | 0100 |
| 19 | 0113 | 262 | 272 | 262 | 240 | 215 | 194 | 171 | 155 | 138 | 126 | 111 | 101 | 0082 |
| 21 | 0098 | 228 | 247 | 241 | 225 | 206 | 187 | 169 | 153 | 140 | 124 | 113 | 103 | 0067 |
| 23 | 0086 | 206 | 227 | 223 | 212 | 194 | 181 | 164 | 149 | 137 | 126 | 114 | 105 | 0058 |
| 25 | 0072 | 184 | 208 | 207 | 197 | 189 | 171 | 161 | 144 | 133 | 122 | 113 | 104 | 0048 |

**Table 2.**

Owing to the slow diminution of the coefficients, the expressions for stress-components are slowly convergent, particularly in the region near the boundary.

Taking a part of the expression for $\sigma_x$, for example, we have from (4), at $x=a/2$ and $y=0$,

$$\frac{\partial^2 F_1}{\partial y^2}=\frac{4P_1}{\pi}\sum_{n=1}^{\infty}\sin\frac{n\pi}{2}A_n$$

The numerical value of this expression is not accurately determined by using $A_n$ for $n$ up to 25, because the values of $A_n$ for $n$ greater than 25 may not be negligibly small as the table suggests. A similar remark applies to $F_2$ and $F_3$, still higher values of $n$ and $s$ than in the present computation will lead to a very tedious calculation.

The stress-components in the central part of the plate are calculated from (1), the results being given in **Table 3** and plotted in **Figs. 20～22.**

As a measure of the accuracy of the above calculations, the sum of $\sigma_y$ from $x=0$ to $x=a$ on the section parallel to the axis of $x$ is measured graphically. The results for a plate of unit thickness are given in the next table, the true value of the numerical coefficient being 0.2, as the applied load is given by $P=0.2ap$.

| Sections | Measured values | Error in % |
|---|---|---|
| $y=0.2\,a$ | $0.2008\,ap$ | +0.4 |
| $0.3\,a$ | $0.2002\,ap$ | −0.1 |
| $0.4\,a$ | $0.1984\,ap$ | −0.8 |
| $0.5\,a$ | $0.1992\,ap$ | −0.4 |

(1) $\sigma_x/P$

| $y/a$ \ $x/a$ | 0.1 | 0.2 | 0.3 | 0.4 | 0.5 |
|---|---|---|---|---|---|
| 0.1 | -0.006 | -0.016 | -0.085 | -0.087 | -0.037 |
| 0.2 | -0.024 | -0.043 | -0.044 | 0.025 | 0.078 |
| 0.3 | -0.014 | -0.016 | 0.012 | 0.062 | 0.085 |
| 0.4 | -0.003 | 0.008 | 0.037 | 0.075 | 0.093 |
| 0.5 | 0 | 0.015 | 0.045 | 0.078 | 0.094 |

(2) $-\sigma_y/P$

| $y/a$ \ $x/a$ | 0.1 | 0.2 | 0.3 | 0.4 | 0.5 |
|---|---|---|---|---|---|
| 0.1 | 0.005 | 0.016 | 0.073 | 0.466 | 0.812 |
| 0.2 | 0.043 | 0.086 | 0.182 | 0.406 | 0.547 |
| 0.3 | 0.072 | 0.124 | 0.222 | 0.348 | 0.411 |
| 0.4 | 0.092 | 0.147 | 0.233 | 0.315 | 0.351 |
| 0.5 | 0.099 | 0.159 | 0.235 | 0.304 | 0.334 |

(3) $\tau/P$

| $y/a$ \ $x/a$ | 0.1 | 0.2 | 0.3 | 0.4 | 0.5 |
|---|---|---|---|---|---|
| 0.1 | 0.016 | 0.098 | 0.124 | 0.259 | 0 |
| 0.2 | 0.020 | 0.059 | 0.130 | 0.195 | 0 |
| 0.3 | 0.016 | 0.050 | 0.084 | 0.074 | 0 |
| 0.4 | 0.012 | 0.027 | 0.039 | 0.031 | 0 |
| 0.5 | 0 | 0 | 0 | 0 | 0 |

(4) $S/P$

| $y/a$ \ $x/a$ | 0.1 | 0.2 | 0.3 | 0.4 | 0.5 |
|---|---|---|---|---|---|
| 0.1 | 0.031 | 0.096 | 0.247 | 0.642 | 0.975 |
| 0.2 | 0.044 | 0.126 | 0.295 | 0.519 | 0.625 |
| 0.3 | 0.067 | 0.147 | 0.288 | 0.436 | 0.496 |
| 0.4 | 0.095 | 0.172 | 0.281 | 0.399 | 0.444 |
| 0.5 | 0.099 | 0.164 | 0.280 | 0.382 | 0.427 |

**Table 3**

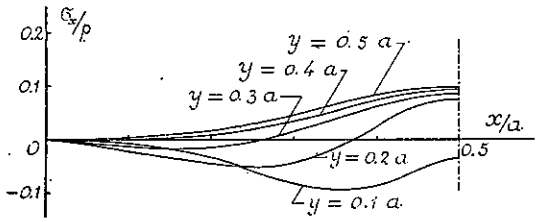


**Fig. 20.**

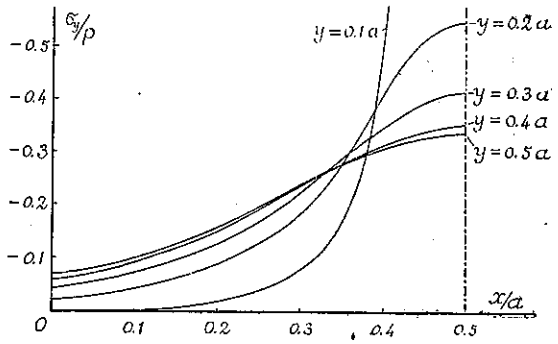


**Fig. 21.**

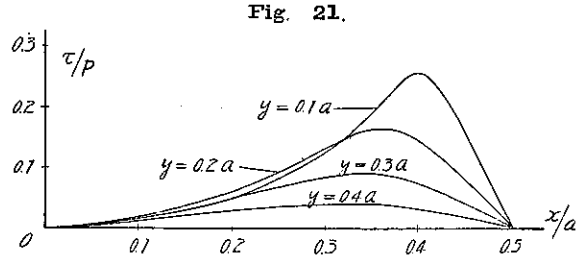


**Fig. 22.**

Thus the measured values are in good agreement with the applied load, showing that the expression for $\sigma_y$ is quite accurate on the sections considered.

The values of the principal stress difference $S$ at various points are calculated in order to trace the isochromatic line, viz.,

$$\frac{S}{p}=\left[\left(\frac{\sigma_x-\sigma_y}{p}\right)^2+\left(\frac{2\tau}{p}\right)^2\right]^{1/2}$$

the result being given in **Table 3.** With the relations $Sd=Kn$ and $P=0.2\,apd$, we have

$$n=\frac{5P}{aK}\frac{S}{p}$$

where $n$ is the order of extinction and $K$ the coefficient of photo-elastic extinction. Taking $P/aK=2$, we get

$$n=10\,S/P$$

This equation enables us to compute the order of extinction at the points where the values of $S/p$ are known. Tracing the loci of the integral values of $n$, we get the theoretical isochromatic lines as shown in **Fig. 23.** Owing to the slow convergency of the expression, the isochromatic lines in the region near the boundary can not be accurately traced.

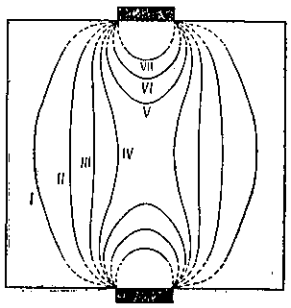


**Fig. 23.**

The determination of the stress distribution near the boundary where the external force acts, is important for drawing isochromatic lines. To meet this desire, we may simplify the problem by considering a semi-infinite plate, of which the boundary is partially subjected to a uniformly distributed pressure, viz. $p$ per unit length of the limited region $AB$, **Fig. 24.**

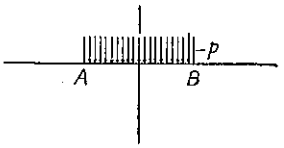


**Fig. 24.**

Such a problem was already dealt with by COKER and FILON[1], and the isochromatic lines are known to be circular arcs passing through $A$ and $B$. Particularly the isochromatic line of the highest order is given by the semi-circle of the diameter $AB$, while the line of the order zero is coincident with the straight line $AB$, of which the two points $A$ and $B$ are to be discarded.

## 16. Experiment.

In order to compare the calculation carried out in the previous article with the experiment, a square plate of phenolite, $33\times33\times6$ mm, was tested under polarized

(1) "*Photo-elasticity*," § 4. 22. p. 352.

light by means of the apparatus described before (**Figs. 10** and **11**). To make the pressure distribution as uniform as possible, a layer of leather strip, 6.6 mm in length, such as used for packing of valves was inserted between the specimen and the compression surface of the machine, and the load of 70 kg was applied through the leather, as shown in **Fig. 25.**

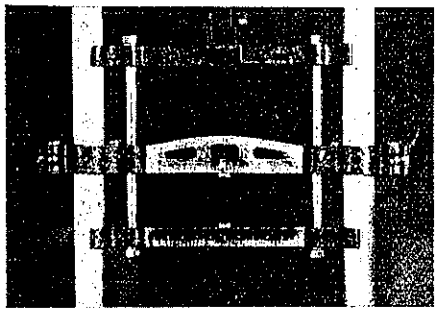

**Fig. 25.**

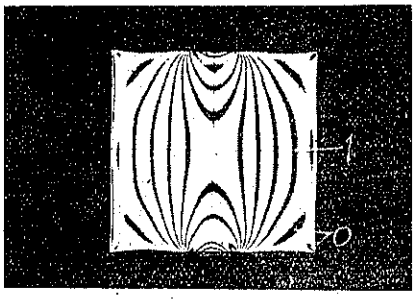


**Fig. 26.**

In the first step the isochromatic lines were photographed at the instant 1 minute after loading (**Fig. 26**). In the present case the load $P$ is 70 kg, and the length of the side of the specimen $a$ is 3.3 cm. The coefficient of photo-elastic extinction $K_1$ being equal to 10.6 kg/cm as shown in the end of Article 3, we have $P/aK_1=2$, which is coincident with the value taken in drawing the theoretical isochromatic lines shown in **Fig. 23.**

Comparing **Fig. 23** with **Fig. 26**, we find that the theoretical and observed lines are in fairly good agreement with each other in the central part of the plate. In the region near the load, the isochromatic lines assemble at the extreme points of the load, as the theory based on uniform surface loading leads one to expect. In addition to such dark bands, there are some other curves which can not be explained on the ground of the present calculation. These curves may be probably due to the variation from the uniform distribution of pressure and also to the presence of initial stress. Along the remaining part of the loaded edges there are thick dark bands, but it is not clear whether they are of the zeroth order of extinction.

The isoclinic lines were then photographed under plane polarized light, **Figs. 27~31** being typical examples. In **Fig. 27**, it is readily found that the principal axes coincide with the horizontal and vertical axes of symmetry, which agrees with the calculation. As COKER and FILON showed in the problem of a semi-infinite plate described before, **Fig. 24**, the theoretical isoclinic lines near the loaded area are known to be rectangular hyperbolas passing through the points $A$, $B$, whose

asymptotes make an angle with the horizontal and vertical which is equal to the inclination of the principal stresses. The isoclinic lines appearing as dark broad bands in **Figs. 28～31** start from the extreme points of the loaded area and bend as the theory suggests.

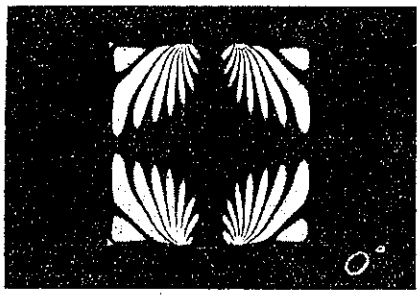


Fig. 27.

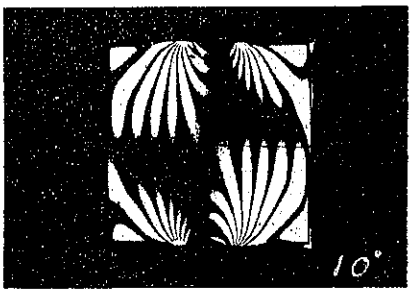


Fig. 28.

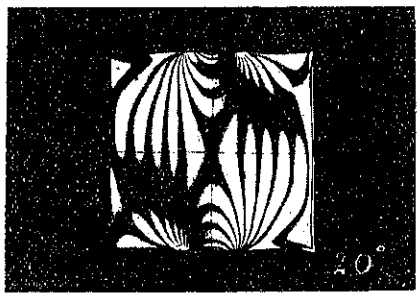


Fig. 29.

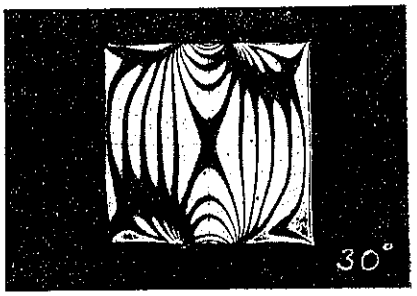


Fig. 30.

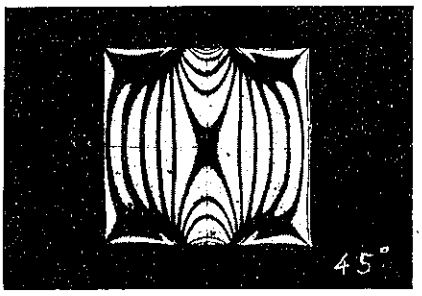


Fig. 31.

## SUMMARY.

(1) If we represent the relation between stress and optical effect in an equation of the form $Sd=K_t n$, the value of $K_t$ varies with the time elapsed after loading. In quantitative analysis of an isochromatic lines, we have to take $K_t$ corresponding to the same duration of time as is observed when we take the line under considera-

tion. At the instant of loading, i. e., $t=0$, $K_0$ for phenolite is 11.0 kg/cm for the green line of the mercury vapour lamp. This figure is found to be much smaller than the values for glass and celluloid, and it is a little smaller than that for bakelite.

**(2)** There is a considerable creep of strain, which follows a law similar to that of the optical effect. So roughly speaking, the optical effect is proportional to strain, i. e., the photo-elastic phenomenon may be interpreted as a result caused by strain.

**(3)** Isochromatic and isoclinic lines theoretically determined for a roller diametrically compressed are shown to be in good agreement in general feature with those obtained experimentally. Isochromatic lines photographed at the instant 15 minutes after loading are found to be greatly different from those taken at one minute after loading.

**(4)** Isochromatic lines in a rectangular plate compressed on two opposite sides are determined by calculation and experiment. Owing to the slow convergency of the series appearing in the expressions for stress-components, particularly in the region near the boundary, the determination of stress in that region can be hardly performed. In the central part of the plate, the calculation is in fairly good agreement with the experiment. For the region near the boundary the result of the calculation of a semi-infinite plate is taken to complete the construction of isochromatic lines.

In conclusion the author wishes to acknowledge his indebtedness to Prof. A. Ono for helpful suggestions and criticisms.